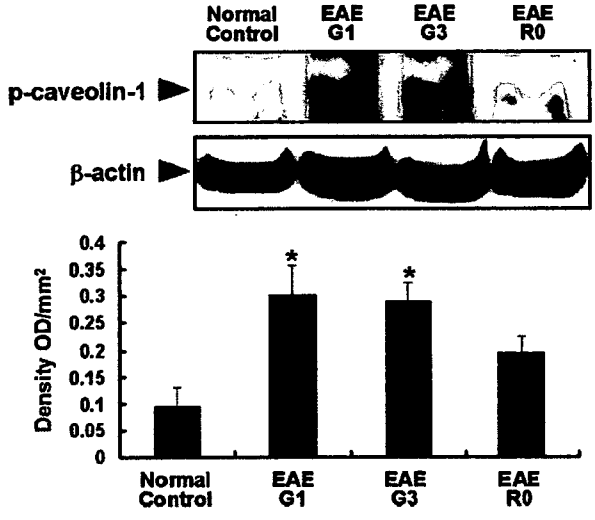

Fig. 1. Western blot using anti-p-caveolin-1 (Tyr-14) antibody in the spinal cords of normal control rats (Normal) and rats in the early (Day 10 p.i.; EAE G1), peak (Day 12 p.i.; EAE G3), and recovery stages of EAE (Day 21 p.i.; EAE R0). Photographs: representative photographs of Western blots for p-caveolin-1 and beta-actin. Arrowheads indicate the positions of p-caveolin-1 (approximately 22 kDa) and beta-actin (45 kDa). Bar graph: the results of densitometric data analysis (mean ± S.E., $n = 5$ rats/group). The relative expression of p-caveolin-1 was calculated after normalization to the beta-actin bands from five different samples. $^{*}p < 0.05$ vs. normal controls.

(density value, 0.095 ± 0.035 OD/mm^2; $n = 5$ rats); it significantly increased in the spinal cord in early (G1, Day 10 p.i.; 0.302 ± 0.056; $n = 5$ rats; $P < 0.05$ versus normal controls) and peak (G3, Day 12 p.i.; 0.292 ± 0.033; $n = 5$ rats; $P < 0.05$) stages of EAE, and it slightly declined in the recovery stage of EAE (R0, Day 21 p.i.; 0.194 ± 0.033; $n = 5$ rats) (Fig. 1).

Immunohistochemically, p-caveolin-1 was constitutively expressed in few vascular endothelial cells and glial cells in the spinal cords of normal rats (Fig. 2A, arrows). In the early stage of EAE (G1, Day 10 p.i.), there was a massive infiltration of inflammatory cells in the subarachnoid space, where round cells were strongly positive for p-caveolin-1 (Fig. 2B, arrowheads). In the peak stage of EAE (Day 12 p.i.), some inflammatory cells and glial cells in the perivascular cuffs were positive for p-caveolin-1 (Fig. 2C). In the recovery stage (Day 21 p.i.), there was decreased perivascular cuffing compared with that in the peak stage; however, a few cells were positive for p-vaceolin-1 (Fig. 2D). In a single immunostaining of p-caveolin-1, immunoreaction of p-caveolin-1 was well-visualized in vascular endothelial cells lining vessels (Fig. 2C and D, marked as "V").

In EAE lesions (Day 12 p.i.), p-caveolin-1 immunoreactivity in the parenchyma was co-localized in some ED1-positive cells, suggesting that macrophages express p-caveolin-1 in the spinal cord with EAE (Fig. 3A–C). p-caveolin-1 (Fig. 3A; inset; red) was co-localized in some OX42-positive ramified microglial cells (Fig. 3B; inset; green) (Fig. 3C; inset; merged). p-caveolin-1 immunoreactivity in the white matter was occasionally co-localized in few GFAP-positive astrocytes, indicating that very few astrocytes expressed p-caveolin-1 immunoreactivity (Fig. 3D–F). As well, a p-caveolin-1-positive reaction in the EAE lesions was seen in some IB4-positive vascular endothelial cells as well as IB4-positive macrophages (Fig. 3G–I). Furthermore, the sections reacted with rabbit anti-p-caveolin-

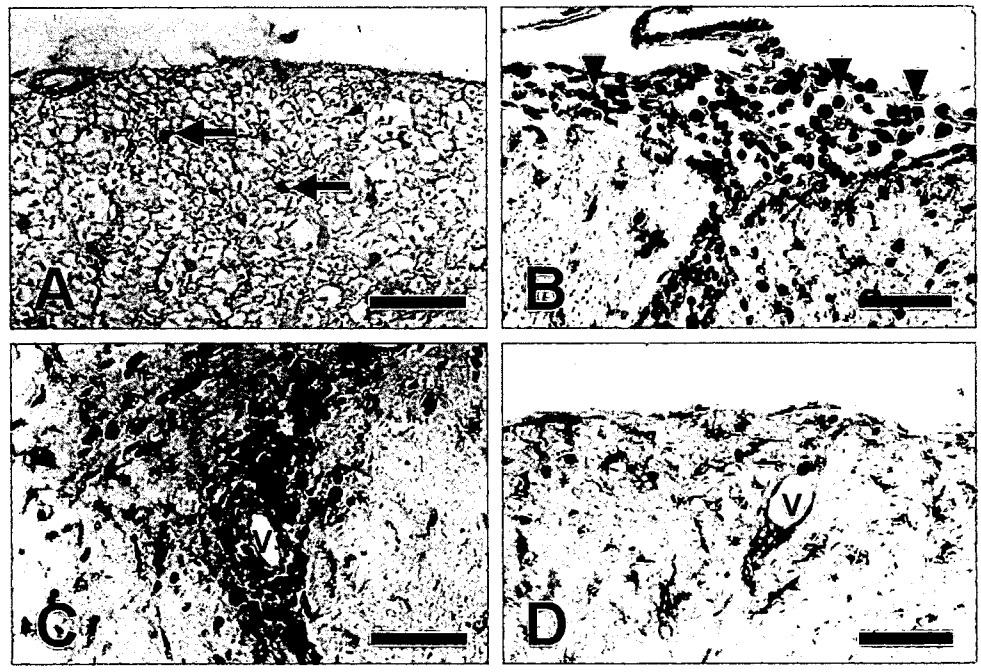

Fig. 2. Immunohistochemical staining of p-caveolin-1 in the spinal cords of normal control rats (A) and rats in the early (B, Day 10 p.i.), peak (C, Day 12 p.i.), and recovery (D, Day 21 p.i.) stages of EAE. P-caveolin-1 was weakly detected in some glial cells in the spinal cords of normal control rats (A, arrows). In the early stage of EAE (B), p-caveolin-1-positive cells were observed in the subarachnoid space (B, arrowheads), whereas glial cells in the white matter showed increased immunoreactivity for p-caveolin-1 (B) compared with controls (A). At the peak stage of EAE (C), the majority of inflammatory cells in perivascular cuffs around a vessel (V) were positive for p-caveolin-1. In the recovery stage of EAE (D), some p-caveolin-1 immunoreactive cells were found. Vascular endothelial cells lining vessels (C and D, marked as "V") were positive for p-caveolin-1. (A–D) counterstained with hematoxylin. Scale bars = 50 μm.

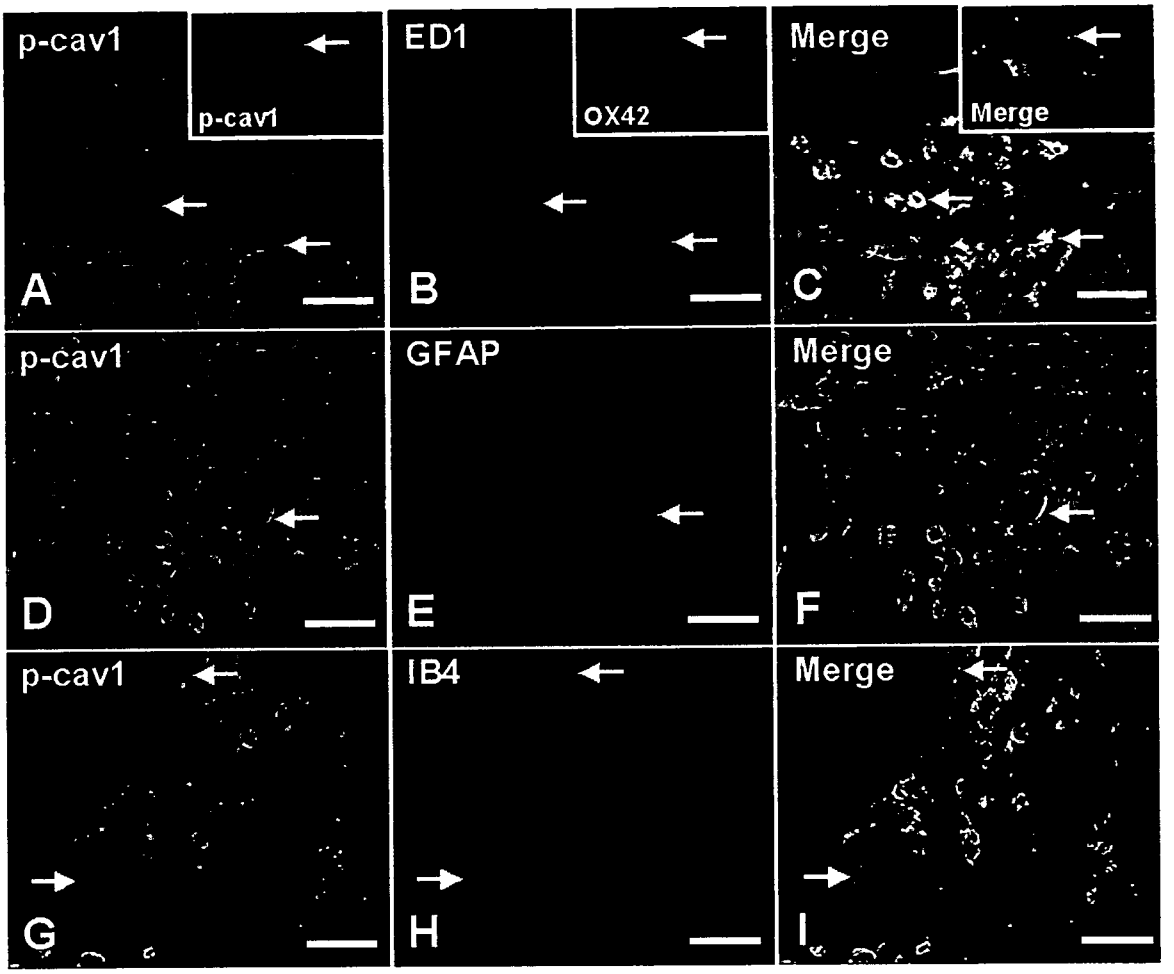

Fig. 3. Identification of p-caveolin-1-positive cells in the spinal cords of Lewis rats with EAE (Day 12 p.i.). The immunoreactivity of p-caveolin-1 (p-cav1) (A, green, arrows) was co-localized in some ED1-positive macrophages (B, red, arrows) in the parenchyma (C, merged, arrows). In insets (A–C), p-caveolin-1 immunoreactivity (A, inset) was co-localized in some OX42-positive cells (B, inset). Arrow in inset (C) shows both positive for p-caveolin-1 and OX42. Some p-caveolin-1-positive cells (D, green, arrow) were positive for GFAP (E, red, arrow) in the white matter (F, merge, arrow). The immunoreactivity of p-caveolin-1 (A, green, arrows) was co-localized in vascular endothelial cells stained for isolectin B4 (IB4) (B, red, arrows) (C, merged, arrows). Scale bars = 30 μm.

1 and either OX1, or R73, p-caveolin-1 immunoreactivity was co-localized in either OX1- or R73-positive cells, suggesting that a majority of inflammatory cells were positive for p-caveolin-1. These findings were matched with those of each single immunostaining as well (data not shown).

In accordance with our previous report that three isoforms of caveolin-1, -2, and -3 increased in EAE lesions [13], we further confirmed that phosphorylation of caveolin occurred in EAE lesions, particularly in the early stage of EAE. This study confirms that the phosphorylation of caveolin-1 in rats with EAE occurs mainly in the inflammatory cells in the subarachnoid space and spinal cord parenchyma, corresponding to the increased expression of caveolin-1 in rats with EAE [13]. However, it is possible that the phosphorylation of caveolin occurs in vascular endothelial cells with EAE, because the immunoreactivity of p-caveolin was enhanced in EAE lesions compared with that in normal controls.

This finding implies that increased phosphorylation of caveolin-1 plays an important role in the pathogenesis of EAE [14]. The biological relevance of caveolin-1 phosphorylation in inflammatory cells and vascular endothelial cells remains to be determined. There is a general consensus that the phosphorylation of caveolin-1 may represent a downstream element of p38 mitogen-activated protein kinase and c-Src in NIH3T3 cells. This is thought to follow stimulation by a variety of cellular stressors, including high osmolarity, hydrogen peroxide, and ultraviolet light [15].

With regard to the fate of inflammatory cells in rat EAE, a majority of inflammatory cells are eliminated through apoptosis owing to the expression of phosphorylated p38 [12]. Matching the two close results described above, it is highly possible that the increased phosphorylation of p38 in inflammatory cells (presumably T cells and macrophages) may stimulate the phosphorylation of caveolin-1 in the spinal cords of rats with EAE, leading to apoptosis of inflammatory cells.

Apart from the role of inflammatory cells in rat EAE, the phosphorylation of caveolin-1 in some astrocytes and neurons remains a topic of debate. We only speculate that increased phosphorylation of caveolin-1 may mediate signal transduction cascades in the affected cells. Recently, it was reported that caveolin-1 phosphorylation is reversible in vascular endothelial cells in vitro [1] and that caveolin-1 is involved in anti-

proliferative activity [6]. If these observations are valid, the increased expression of caveolin-1 in rat spinal cords with EAE is reduced reversibly in the recovery stage of EAE and is partly involved in anti-proliferation in astrocytes as well as other inflammatory cells. In fact, the proliferation of inflammatory cells and glial cells was found to be very limited when present [14]. Based on current knowledge, we postulate that the phosphorylation of caveolin-1 occurred in the inflammatory cells, particularly in the subarachnoid space and parenchyma of spinal cords with EAE, and mediated the cell death signal cascades in inflammatory cells. In the spinal cord parenchyma with EAE at the peak and recovery stages, the phosphorylation of caveolin-1 was reduced and/or reversed and contributed to the suppression of glial cell proliferation.

Acknowledgment

This work was supported by a Korea Research Foundation Grant through funding from the Korean Government (MOEHRD) (KRF-2005-041-E00402).

References

[1] D.B. Chen, S.M. Li, X.X. Qian, C. Moon, J. Zheng, Tyrosine phosphorylation of caveolin 1 by oxidative stress is reversible and dependent on the c-src tyrosine kinase but not mitogen-activated protein kinase pathways in placental artery endothelial cells, Biol. Reprod. 73 (2005) 761–772.

[2] F. Galbiati, D. Volonte, O. Gil, G. Zanazzi, J.L. Salzer, M. Sargiacomo, P.E. Scherer, J.A. Engelman, A. Schlegel, M. Parenti, T. Okamoto, M.P. Lisanti, Expression of caveolin-1 and -2 in differentiating PC12 cells and dorsal root ganglion neurons: caveolin-2 is up-regulated in response to cell injury, Proc. Natl. Acad. Sci. U.S.A. 95 (1998) 10257–10262.

[3] P. Gargalovic, L. Dory, Cellular apoptosis is associated with increased caveolin-1 expression in macrophages, J. Lipid Res. 44 (2003) 1622–1632.

[4] J. Harris, D. Werling, J.C. Hope, G. Taylor, C.J. Howard, Caveolae and caveolin in immune cells: distribution and functions, Trends Immunol. 23 (2002) 158–164.

[5] T. Ikezu, H. Ueda, B.D. Trapp, K. Nishiyama, J.F. Sha, D. Volonte, F. Galbiati, A.L. Byrd, G. Bassell, H. Serizawa, W.S. Lane, M.P. Lisanti, T. Okamoto, Affinity-purification and characterization of caveolins from the brain: differential expression of caveolin-1, -2, and -3 in brain endothelial and astroglial cell types, Brain Res. 804 (1998) 177–192.

[6] H.P. Kim, X. Wang, A. Nakao, S.I. Kim, N. Murase, M.E. Choi, S.W. Ryter, A.M. Choi, Caveolin-1 expression by means of p38 beta mitogen-activated protein kinase mediates the anti-proliferative effect of carbon monoxide, Proc. Natl. Acad. Sci. U.S.A. 102 (2005) 11319–11324.

[7] A.L. Kiss, A. Turi, N. Muller, O. Kantor, E. Botos, Caveolae and caveolin isoforms in rat peritoneal macrophages, Micron 33 (2002) 75–93.

[8] S. Li, T. Okamoto, M. Chun, M. Sargiacomo, J.E. Casanova, S.H. Hansen, I. Nishimoto, M.P. Lisanti, Evidence for a regulated interaction between heterotrimeric G proteins and caveolin, J. Biol. Chem. 270 (1995) 15693–15701.

[9] S. Li, R. Seitz, M.P. Lisanti, Phosphorylation of caveolin by src tyrosine kinases. The alpha-isoform of caveolin is selectively phosphorylated by v-Src in vivo, J. Biol. Chem. 271 (1996) 3863–3868.

[10] T. Okamoto, A. Schlegel, P.E. Scherer, M.P. Lisanti, Caveolins, a family of scaffolding proteins for organizing "preassembled signaling complexes" at the plasma membrane, J. Biol. Chem. 273 (1998) 5419–5422.

[11] C.S. Raine, The Dale E. McFarlin Memorial Lecture: the immunology of the multiple sclerosis lesion, Ann. Neurol. 36 (Suppl.) (1994) S61–S72.

[12] T. Shin, M. Ahn, K. Jung, S. Heo, D. Kim, Y. Jee, Y.K. Lim, E.J. Yeo, Activation of mitogen-activated protein kinases in experimental autoimmune encephalomyelitis, J. Neuroimmunol. 140 (2003) 118–125.

[13] T. Shin, H. Kim, J.K. Jin, C. Moon, M. Ahn, N. Tanuma, Y. Matsumoto, Expression of caveolin-1, -2, and -3 in the spinal cords of Lewis rats with experimental autoimmune encephalomyelitis, J. Neuroimmunol. 165 (2005) 11–20.

[14] T. Shin, T. Kojima, N. Tanuma, Y. Ishihara, Y. Matsumoto, The subarachnoid space as a site for precursor T cell proliferation and effector T cell selection in experimental autoimmune encephalomyelitis, J. Neuroimmunol. 56 (1995) 171–178.

[15] D. Volonte, F. Galbiati, R.G. Pestell, M.P. Lisanti, Cellular stress induces the tyrosine phosphorylation of caveolin-1 (Tyr(14)) via activation of p38 mitogen-activated protein kinase and c-Src kinase. Evidence for caveolae, the actin cytoskeleton, and focal adhesions as mechanical sensors of osmotic stress, J. Biol. Chem. 276 (2001) 8094–8103.

[16] H. Yamada, E. Yamada, A. Higuchi, M. Matsumura, Retinal neovascularisation without ischaemia in the spontaneously diabetic Torii rat, Diabetologia 48 (2005) 1663–1668.

BRAIN RESEARCH 1102 (2006) 86–91

available at www.sciencedirect.com

SCIENCE DIRECT®

www.elsevier.com/locate/brainres

BRAIN RESEARCH

Short Communication

Immunohistochemical study of caveolin-1 in the sciatic nerves of Lewis rats with experimental autoimmune neuritis

Meejung Ahn[a], *Changjong Moon*[a], *Heechul Kim*[a], *Jeeyoung Lee*[a], *Chang Sung Koh*[b], *Yoh Matsumoto*[c], *Taekyun Shin*[a,*]

[a]*Department of Veterinary Medicine, Cheju National University, Jeju 690-756, South Korea*
[b]*Department of Medical Technology, School of Allied Medical Science, Shinshu University, Matsumoto, Japan*
[c]*Department of Molecular Neuropathology, Tokyo Metropolitan Institute for Neuroscience, Fuchu, Tokyo, Japan*

ARTICLE INFO

Article history:
Accepted 8 May 2006
Available online 23 June 2006

Keywords:
Caveolin-1
Demyelination
Experimental autoimmune neuritis
PNS

Abbreviations:
eNOS, endothelial nitric oxide synthase
EAN, experimental autoimmune neuritis
MAP, mitogen-activated protein
PNS, peripheral nervous system

ABSTRACT

The expression of caveolin-1 and the related molecule endothelial nitric oxide synthase (eNOS) was analyzed in the sciatic nerves of Lewis rats with experimental autoimmune neuritis (EAN). Western blot analysis showed that caveolin-1 significantly increased in the sciatic nerves with EAN upon initiation of cell infiltration during the early and peak stages (days 10 and 14 post-immunization, p.i.) and declined thereafter. The pattern of eNOS expression over the course of EAN largely matched that of caveolin-1. Immunohistochemistry showed that in EAN lesions, intense caveolin-1 immunostaining occurred in ED1-positive macrophages as well as in vessels, while the caveolin-1 immunoreaction was reduced in Schwann cells in the inflammatory lesions. Consequently, we postulated that caveolin-1 expression increased in the sciatic nerves with EAN; this possibly mediated either molecular trafficking or nitric oxide generation partly through the activation of eNOS in vascular endothelial cells, as well as in inflammatory macrophages in EAN and/or cellular apoptosis of inflammatory cells.

Caveolin-1 is one of the structural proteins of caveolae, which are flask-shaped vesicular invaginations of the plasma membrane with diameters of 50 to 100 nm (Ikezu et al., 1998; Okamoto et al., 1998). Caveolin is a transmembrane adaptor molecule that recognizes GPI-linked proteins and interacts with downstream cytoplasmic signaling molecules, such as Src-family tyrosine kinases and hetero-trimeric G proteins. Caveolin is abundant in a variety of cell types, including adipocytes, endothelial cells, smooth muscle cells (Okamoto et al., 1998), macrophages (Kiss et al., 2002), and astrocytes (Shin et al., 2005), where it possibly mediates signal transduction.

Mechanistically, caveolins interact with a variety of downstream signaling molecules, including Src-family tyrosine kinases, p42/44 mitogen-activated protein (MAP) kinase, and endothelial nitric oxide synthase (eNOS), and hold these signal transducers in an inactive conformation until

* *Corresponding author.* Fax: +82 64 756 3354.
E-mail address: shint@cheju.ac.kr (T. Shin).

0006-8993/$ – see front matter © 2006 Elsevier B.V. All rights reserved.
doi:10.1016/j.brainres.2006.05.044

activation by an appropriate stimulus (Williams and Lisanti, 2004). When cells are activated by calcium ions, the bound eNOS and caveolin in the plasma membrane dissociate, and eNOS may stimulate the production of nitric oxide in the affected cells. Therefore, over-expression of caveolin-1 in fibroblasts and epithelial cells is reported to sensitize these cells to apoptotic stimuli, possibly via the direct or indirect activation of caspase-3 (Liu et al., 2001). Although caveolin-1 participates in myelination of the sciatic nerve (Mikol et al., 2002), little is known about the involvement of caveolins in pathological processes of the peripheral nervous system (PNS), such as in the sciatic nerve.

Experimental autoimmune neuritis (EAN), an animal model of human demyelinating diseases, is a neuritogenic, antigen-responsive, CD4+, T cell-mediated, autoimmune PNS disease, which is characterized by the infiltration of T cells and bystander macrophages into peripheral nerves, including the sciatic nerve, leading to hindlimb paralysis (Conti et al., 2004; Weishaupt et al., 2001; Zetti et al., 1996; Zhu et al., 2004). In the rat EAN model, the majority of inflammatory cells in EAN lesions were eliminated via apoptosis (Conti et al., 1998; Lee and Shin, 2002; Moon et al., 2005; Zetti et al., 1996). During the course of EAN, many inflammatory mediators, such as cytokines (Zhu et al., 2004), cyclooxygenases (Shin et al., 2003), osteopontin (Ahn et al., 2004a), and NOS (Conti et al., 2004; Lee and Shin, 2002) are involved in the initiation or recovery of EAN paralysis. Furthermore, we previously found that mitogen-activated protein kinases, including extracellular signal regulated kinases (Ahn et al., 2004b) and p38 (Moon et al., 2005), are activated in a variety of cells in EAN lesions, and these also are related to caveolins (Williams and Lisanti, 2004). Considering the previous findings in EAN models, it is likely that caveolin-1 expression is affected in the pathogenesis of EAN because caveolins are among the important plasma membrane proteins in inflammatory cells and Schwann cells in EAN lesions.

This study examined whether the expression of caveolin-1 was affected in the sciatic nerves of Lewis rats with EAN and investigated the relationship between caveolin-1 and eNOS in EAN lesions.

Lewis rats were obtained from Harlan (Sprague–Dawley, Indianapolis, IN) and bred in our animal facility. Thirty male rats aged 7–12 weeks and weighing 160–200 g were used in the experiments. The animals were housed in cages in a standard barrier facility and maintained on a 12-h light:12-h dark cycle at 23 °C. The research was conducted in accordance with the internationally accepted principles for laboratory animal use and care as found in the NIH guidelines (Bethesda, MD). Active EAN was induced in the Lewis rats, as described previously (Ahn et al., 2004a,b). Each rat was injected in both hind footpads with an emulsion containing 100 μg of SP26 (a neuritogenic peptide homologous to amino acids 53–78 of bovine myelin P2 protein (Shimadzu, Kyoto, Japan)) and CFA (*M. tuberculosis* H37Ra, 5 mg/ml) and was evaluated clinically, as reported previously (Lee and Shin, 2002). Each rat was treated with 50 ng of pertussis toxin (Sigma, St. Louis, MO) on days 0 and 2 after immunization. The progress of EAN was divided into seven clinical stages: Grade (G) 0, no signs; G1, floppy tail; G2, mild paraparesis; G3, severe paraparesis; G4, tetraparesis; G5, moribund condition or death; and R0, the recovery stage. Adjuvant control rats were immunized with CFA only.

To study the expression of caveolin-1 in Lewis rats with EAN, tissues were sampled (n = 6 per time point) on post-immunization (p.i.) days 10 (early stage), 14 (peak stage), 21, and 30 (recovery stage) of EAN. Age-matched rats (n = 6) were used as controls. The sciatic nerves were removed and frozen at −70 °C for protein analysis. Pieces of sciatic nerve were embedded in paraffin after fixation in 4% paraformaldehyde in phosphate-buffered saline (PBS), pH 7.4.

The specificity of rabbit polyclonal anti-caveolin-1 (N-20) (Santa Cruz Biotechnologies, Santa Cruz, CA) has been well characterized by the manufacturer. It was an affinity purified rabbit antibody raised against a peptide mapping at the N-terminus of caveolin-1 of human origin in the data sheet supplied by the manufacturer. Mouse monoclonal anti-eNOS (cat. #N-30020) was obtained from BD Transduction Laboratories (San Diego, CA), which was raised against amino acid 1025–1203 mapping at the C-terminus of eNOS of human vascular endothelium origin. Moreover, eNOS antibody has been routinely tested by Western blot analysis using a positive control (human vascular endothelial cells). Mouse monoclonal anti-β-actin was obtained from Sigma. ED1 (mouse monoclonal anti-rat CD68 antibody) (Serotec, London, UK) was used to detect macrophages.

The sciatic nerves were homogenized in lysis buffer (40 mM Tris, 120 mM NaCl, 0.1% Nonidet 40, 2 Na_3VO_4, 1 mM phenylmethylsulfonyl fluoride, 10 μg/ml aprotinin, and 10 μg/ml leupeptin) with 20 strokes in a homogenizer. The homogenates were transferred into microtubes and centrifuged at 12,000 rpm for 20 min, and then the supernatant was harvested.

For the immunoblot assay, supernatant containing 40 μg of protein was loaded into each lane of a 10% SDS-PAGE gel and electrophoresed; the protein bands were then immunoblotted onto nitrocellulose membrane (Bio-Rad, Hercules, CA). The residual binding sites on the membrane were blocked by incubation with 5% nonfat milk in Tris-buffered saline (TBS) (10 mM Tris–HCl, pH 7.4, and 150 mM NaCl) for 1 h, and then the membrane was incubated for 2 h with the primary reagents, including polyclonal anti-caveolin-1 (1:1000) or monoclonal anti-eNOS (1:1000) antibodies. The blots were washed three times in TBS containing 0.1% Tween-20 and probed with appropriate secondary antibodies, including horseradish peroxidase-conjugated goat anti-rabbit IgG or anti-mouse IgG (Vector, Burlingame, CA) for 1 h. The blots were developed using enhanced chemiluminescence (ECL) reagents according to the manufacturer's instructions. After visualization with ECL, the antibodies were stripped from the membrane, and it was reprobed with mouse monoclonal anti-β-actin antibody (Sigma). The density of each band obtained in the Western blot analysis was measured with a scanning laser densitometer (GS-700; Bio-Rad) and was analyzed using Molecular Analyst software (Bio-Rad). The ratio of caveolin-1 to beta-actin was compared. The results were analyzed statistically using one-way analysis of variance (ANOVA) followed by the Newman–Keuls test. In all cases, $p < 0.05$ was considered significant.

After deparaffinization and hydration, the sections were treated with 0.3% hydrogen peroxide in methyl alcohol for

30 min to block endogenous peroxidase. Some paraffin sections used for caveolin-1 immunostaining were boiled in 10 mM sodium citrate (pH 6.0) for 10 min at 95 °C.

After three washes with PBS, the sections were exposed to 10% normal goat serum and then incubated with rabbit polyclonal anti-caveolin-1 (1:400). After three washes, the appropriate biotinylated secondary antibody and the avidin–biotin–peroxidase complex (ABC) from the Elite kit (Vector) were added sequentially. Peroxidase was developed with a diaminobenzidine tetrahydrochloride (DAB) substrate kit (Vector). The sections were counterstained with hematoxylin before being mounted.

For double staining of two antigens in the same section, double immunofluorescence was applied using fluorescein isothiocyanate (FITC)-labeled goat anti-rabbit IgG (1:50 dilution; Sigma) and tetramethyl rhodamine isothiocyanate (TRITC)-labeled goat anti-mouse IgG (1:50 dilution; Sigma) secondary antibodies to co-localize either caveolin-1 and ED1 or eNOS in the same cell.

DNA fragmentation was detected using in situ nick end-labeling (terminal deoxynucleotidyl transferase (TdT)-mediated dUTP nick end-labeling, TUNEL), performed according to the manufacturer's instructions (ApopTag® In Situ Apoptosis Detection kit; Intergen, Purchase, NY). Co-localization of the TUNEL reaction and caveolin-1 immunoreactivity was examined by double immunofluorescent labeling in the same section. In brief, after the TUNEL reaction, which had been incubated with TRITC-labeled anti-digoxigenin antibody, a second immunofluorescent label was applied using FITC-labeled goat anti-rabbit IgG (1:50 dilution; Sigma) secondary antibody to co-localize the TUNEL reaction and each protein antigen in the same cell.

Fig. 1 shows the pattern of caveolin-1 expression in the sciatic nerves of normal and EAN rats. The expression of caveolin-1 increased significantly in the sciatic nerve in EAN at the early (day 10 p.i.) and peak stages (day 14 p.i.) compared with the expression in normal controls (threefold increase; $p < 0.001$, $n = 3$/each time point), whereas the expression of caveolin-1 declined slightly in the recovery stage (days 21 and 30 p.i.). The level of caveolin-1 in the sciatic nerves of rats recovering from EAN was still higher than that of normal controls, suggesting that many cells in the EAN-affected sciatic nerves still contained increased levels of caveolin-1, although the rats had recovered from paralysis at days 21 and 30 p.i. The Western blot data suggest that caveolin-1 is expressed constitutively in the normal sciatic nerves of rats and that caveolin-1 is increased temporarily in the inflammatory lesion in the sciatic nerves with EAN. Caveolin-1 is in intimate contact with eNOS in the plasma membrane, and eNOS is increased in the sciatic nerves in EAN rats (Lee and Shin, 2002). Therefore, in this study, we examined whether both antigens are affected in EAN tissues.

Fig. 2 shows the pattern of eNOS expression in the sciatic nerves of normal and EAN rats. The level of eNOS expression increased significantly in the sciatic nerve with EAN at the early (day 10 p.i.) and peak (day 14 p.i.) stages compared with the expression in normal controls (greater than threefold increase; $p < 0.001$), and the expression of eNOS declined significantly in the recovery stage (days 21 and 30 p.i.). These

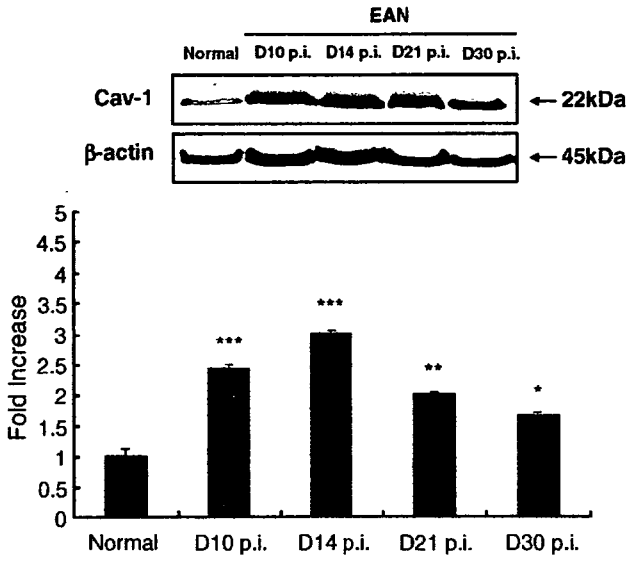

Fig. 1 – A representative Western blot analysis of caveolin-1 and β-actin in the sciatic nerves of normal control rats (normal control) and EAN rats (days 10, 14, 21, and 30 p.i.). A single band was seen with the approximate molecular weight of caveolin-1 (22 kDa). The β-actin level is shown in the same blot. The bar graph shows a significant increase in caveolin-1 immunoreactivity in the sciatic nerves in EAN at the early (day 10 p.i.) and peak stages (day 14 p.i.), whereas its level declined gradually during the recovery stage (days 21 and 30 p.i.); however, caveolin-1 expression during the recovery stage still remained higher than in normal controls. ***$P < 0.001$, ** $P < 0.01$, *$P < 0.05$ vs. normal controls.

results indicate that the pattern of eNOS expression in EAN is similar to that of caveolin-1 in the early and peak stages of EAN, suggesting that eNOS has an intimate relationship with caveolin-1 at the time of initiation of PNS inflammation in the rat EAN model.

In normal sciatic nerves, caveolin-1 was detected in some vascular endothelial cells and some Schwann cells (Fig. 3A). At the peak stage of EAN (day 14 p.i.), some inflammatory cells in the EAN lesions were positive for caveolin-1, while the caveolin-1 immunoreaction was reduced in Schwann cells in the inflammatory lesions (Fig. 3B). At this stage of EAN, caveolin-1 expression was enhanced in vascular endothelial and smooth muscle cells in the tunica media of vessels (Fig. 3B). As negative controls, the primary antisera were omitted or normal rabbit antiserum was substituted for a few tissue sections in each experiment; no specific labeling of the cells was found in these sections (data not shown).

In a double-labeling experiment, caveolin-1 immunoreactivity (Fig. 4A) was mainly detected in ED1-positive macrophages (Fig. 4B) in the same section (Fig. 4C, merge). Macrophages are one of the major inflammatory cells in EAN lesions. Caveolin-1 was also immunostained in small round cells, identical to T cells, in frozen sections (data not shown). These findings suggest that the majority of inflammatory cells as well as host Schwann cells temporarily express caveolin-1 in EAN lesions.

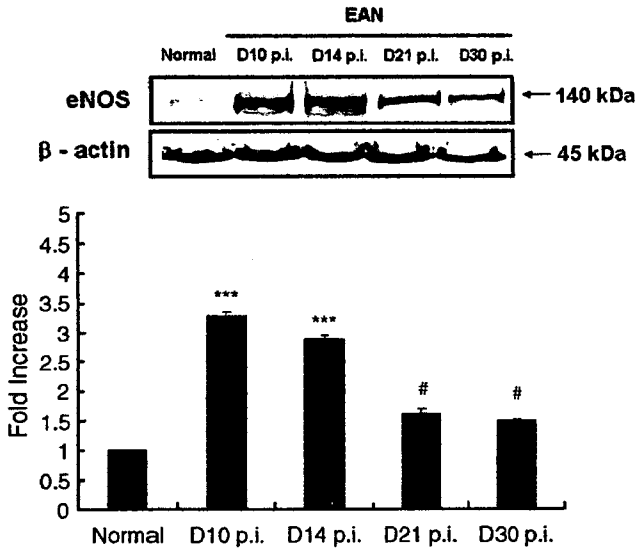

Fig. 2 – A representative Western blot analysis of eNOS and β-actin in the sciatic nerves of normal control rats (normal control) and EAN rats (days 10, 14, 21, and 30 p.i.). A single band was seen at the approximate molecular weight of eNOS (140 kDa). The β-actin level is shown in the same blot. The bar graph shows a significant increase in eNOS immunoreactivity in the sciatic nerves in EAN at the early stage (day 10 p.i.) that persisted at the peak stage (day 14 p.i.) compared with that in normal control sciatic nerves; the eNOS level declined significantly at the recovery stage (days 21 and 30 p.i.). ***$P < 0.001$ vs. normal controls. #$P < 0.05$ vs. D 10 PI and D 14 PI.

The majority of Schwann cells have been found to express eNOS in EAN lesions (Lee and Shin, 2002). To examine whether caveolin-1 and eNOS were both expressed in the same cells, we performed double labeling.

Both caveolin-1 (Fig. 5A, arrows) and eNOS (Fig. 5B, arrows) were immunostained in the same Schwann cell in EAN lesions (Fig. 5C, merge, arrows), suggesting that the two molecules have an intimate relationship within the same cell, as reported in a review article (Williams and Lisanti, 2004).

The expression of caveolin-1 in apoptotic cells in EAN was examined to see the involvement of caveolin-1 in the elimination of inflammatory cells in EAN. Some cells, which were identical to macrophages morphologically, were both positive for caveolin-1 (Fig. 5D) and TUNEL (Figs. 5E and F, merge), suggesting that some apoptotic cells express caveolin-1.

This is the first confirmation that caveolin-1 expression is altered in the sciatic nerve during the course of EAN. Many studies have suggested that caveolin-1 is expressed constitutively in Schwann cells, is up-regulated at the time of myelination, and decreases when Schwann cells lose contact with axons, i.e., axotomy (Mikol et al., 2002). This implies that the constant level of caveolin-1 in Schwann cells is essential for the maintenance of myelin–axon contact.

In EAN, we found a marked increase of caveolin-1 in the affected sciatic nerves and confirmed that the majority of inflammatory macrophages expressed caveolin-1. This suggests that macrophages are activated, in part, via the increased expression of caveolin-1, at least in EAN. We do not exclude the possibility that some vessels also have increased expression of caveolin-1.

The functional role of caveolin-1 in Schwann cells in EAN remains unclear. We postulate that the majority of Schwann cells expressing caveolin-1 in EAN are in contact with axons and consequently continue to express caveolin-1, just as Schwann cells in normal rats do. It is also possible that Schwann cells with decreased caveolin-1 expression proliferate in focal EAN demyelination lesions, as they do in axotomy (Mikol et al., 2002).

Although many factors may influence the expression of caveolin-1 in Schwann cells, hyperglycemia is known to decrease the caveolin-1 level in Schwann cells (Tan et al., 2003). In an animal model of type 1 diabetes, hyperglycemia induced a progressive decrease of caveolin-1 in Schwann cells of the sciatic nerve that was reversed by insulin therapy (Tan et al., 2003). Moreover, hyperglycemia prolonged the kinetics of Erb B2 phosphorylation and significantly enhanced the

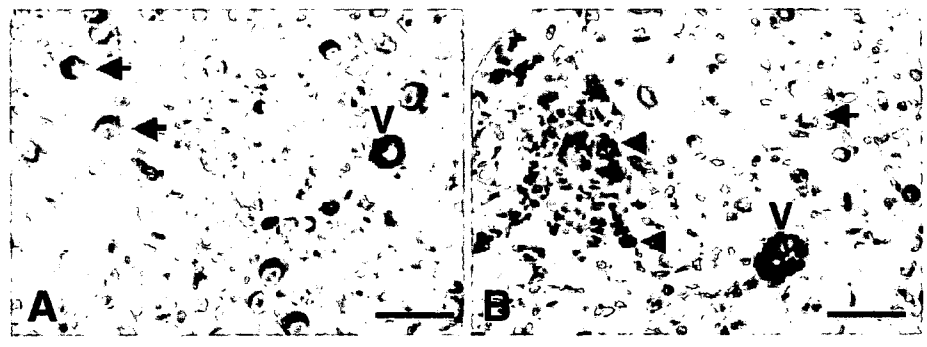

Fig. 3 – Immunohistochemical staining of caveolin-1 in the sciatic nerves of normal control (A) and EAN rats at the peak stage (day 14 p.i.; grade 3) (B). In the normal control sciatic nerves, caveolin-1 was detected in some vessels (A, "V") and some Schwann cells (A, arrows). At the peak stage of EAN (day 14 p.i.), caveolin-1 was reduced in some Schwann cells (B, arrow). Some inflammatory cells (B, arrowheads) and some vessels (B, "V") in the sciatic nerves were positive for caveolin-1 with increased immunoreactivity (B). (A and B) Counterstained with hematoxylin. Scale bars = 30 μm.

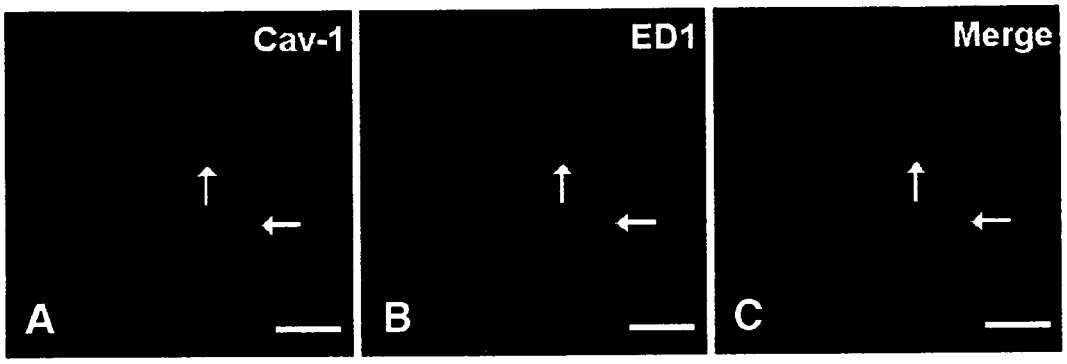

Fig. 4 – Double immunofluorescence of caveolin-1 (A) with ED1 (B) in the sciatic nerve in EAN (day 14 p.i.; grade 3). Caveolin-1-positive reaction (A, green, arrows) in the sciatic nerve was seen mainly in ED1-positive (B, red, arrows) activated macrophages in the same section. Panel C showed a merged image. (A–C) Scale bars = 30 μm. (For interpretation of the references to colour in this figure legend, the reader is referred to the web version of this article.)

mitogenic response of Schwann cells to neuregulin-1-β1, and this effect was mimicked by the forced down-regulation of caveolin-1 (Tan et al., 2003). These findings suggest that the down-regulation of caveolin-1 in diabetes stimulates the Schwann cells to proliferate or differentiate via the binding neuregulin-1 with its receptor, Erb B2.

The majority of Schwann cells remain in EAN, although some axons are demyelinated in EAN lesions. Therefore, it is possible that the expression of caveolin-1 was repressed in Schwann cells that underwent demyelination in focal lesions. Even in the presence of factors that decrease the expression of caveolin-1 in EAN, such as demyelination, we found increased caveolin-1 expression in EAN lesions in this study. We postulate that increased caveolin-1 expression in inflammatory cells, probably macrophages, overwhelms the decreased expression of caveolin-1 in some Schwann cells, if any.

Caveolins are multifunctional in many different cell types and interact with a variety of downstream signaling

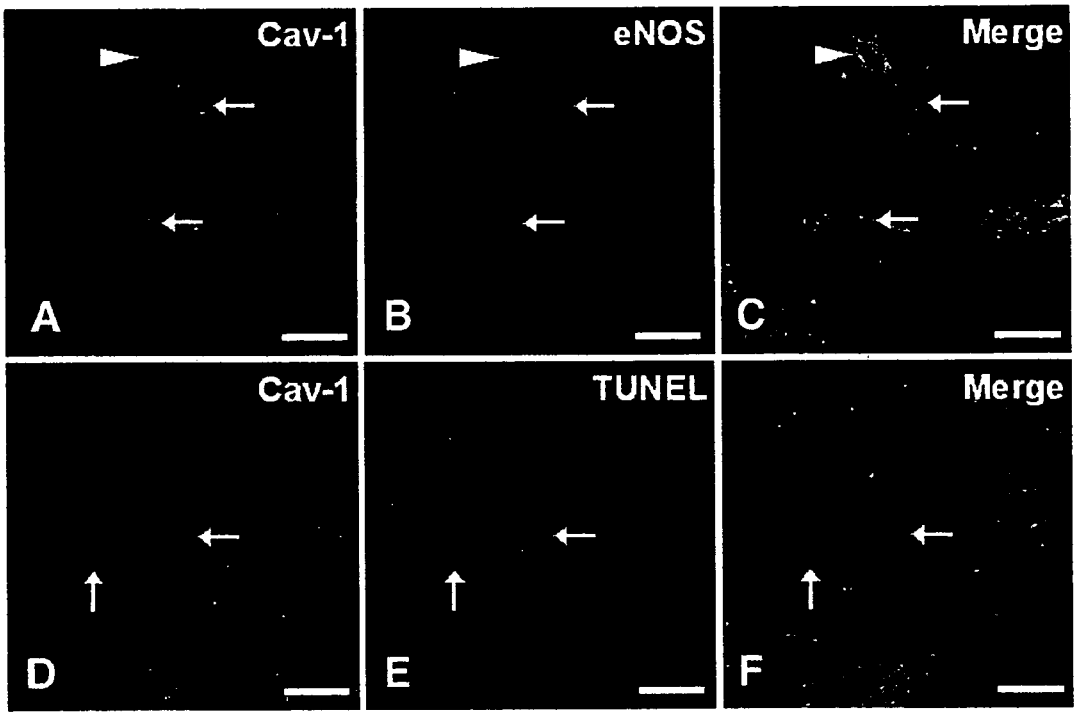

Fig. 5 – Double immunofluorescence of caveolin-1 (A, D) with endothelial NOS (eNOS) (B) and terminal deoxynucleotidyl transferase (TdT)-mediated dUTP nick end-labeling (TUNEL) (E) in the sciatic nerve in EAN (day 14 p.i.; grade 3) (A–F). Both caveolin-1 (A, green, arrows) and eNOS (B, red, arrows) were immunostained in the same section (C, merge, arrows). Arrows indicate caveolin-1 and eNOS-positive Schwann cells, while an arrowhead indicates a vessel that was positive for both caveolin-1 and eNOS (C). Caveolin-1 was mainly localized in the cellular membrane (D, green, arrows), while TUNEL reaction was localized in nuclei (E, red, arrows) (F, merge, arrows). (A–F) Scale bars = 30 μm. (For interpretation of the references to colour in this figure legend, the reader is referred to the web version of this article.)

molecules, including Src-family tyrosine kinases, p42/44 mitogen-activated protein (MAP) kinase, endothelial nitric oxide synthase, and caspase-3, holding these signal transducers in the inactive conformation until activation by an appropriate stimulus (Williams and Lisanti, 2004). We found previously that Schwann cells in EAN up-regulated the expression of both eNOS (Lee and Shin, 2002) and MAP kinases (Ahn et al., 2004b; Moon et al., 2005). Although we did not examine the direct effect of caveolin-1 in Schwann cells in rat EAN in this study, it is possible that caveolin-1 plays a role in the activation of eNOS, or vice versa. Furthermore, caveolin-1 may stimulate caspase-3 and MAP kinases, possibly contributing to the generation of nitric oxide and cell survival, as postulated previously (Ahn et al., 2004b).

Concerning the involvement of caveolin-1 in apoptosis in EAN lesions, it would be one of many death-related factors. The majority of Schwann cells in the EAN model survive, although 10% of Schwann cells die via apoptosis (Conti et al., 2004). By contrast, the majority of inflammatory T cells and macrophages are eliminated via apoptosis during the recovery stage of EAN (Lee and Shin, 2002; Zetti et al., 1996). T cells lack caveolin-1, but caveolins may play an important role in macrophages in EAN. Caveolin-1 has been implicated in the apoptosis of macrophages (Gargalovic and Dory, 2003). If this is the case, we postulate that macrophages in EAN lesions undergo apoptosis, in part, via the expression of caveolin-1. In agreement with these previous studies, we hypothesize that, in EAN lesions, some Schwann cells, which over-express caveolin-1, die via apoptosis when activated by inflammatory cells. This postulate is further supported by the finding that caveolin-1 can act as a coupling or sensitizing factor in signaling apoptotic cell death in both fibroblastic (NIH/3T3) and epithelial (T24) cells through the activation of caspase-3 (Liu et al., 2001).

Consequently, we propose that caveolin-1 increases in EAN lesions and that caveolin-1 in some cell types, including macrophages, is involved in the process of apoptosis. Moreover, we suggest that caveolin-1 in Schwann cells in our autoimmune peripheral nervous system disease model is involved in the signal transduction pathway that includes nitric oxide synthase.

Acknowledgment

This work was supported by Grant R01-2002-000-00053-0 (2004) from the Basic Research Program of the Korea Science and Engineering Foundation.

REFERENCES

Ahn, M., Lee, Y., Moon, C., Jin, J.K., Matsumoto, Y., Koh, C.S., Kim, H.M., Shin, T., 2004a. Upregulation of osteopontin in Schwann cells of the sciatic nerves of Lewis rats with experimental autoimmune neuritis. Neurosci. Lett. 372, 37–141.

Ahn, M., Moon, C., Lee, Y., Koh, C.S., Kohyama, K., Tanuma, N., Matsumoto, Y., Kim, H.M., Kim, S.R., Shin, T., 2004b. Activation of extracellular signal-regulated kinases in the sciatic nerves of rats with experimental autoimmune neuritis. Neurosci. Lett. 372, 57–61.

Conti, G., Scarpini, E., Rostami, A., Livraghi, S., Baron, P.L., Pleasure, D., Scarlato, G., 1998. Schwann cell undergoes apoptosis during experimental allergic neuritis (EAN). J. Neurol. Sci. 161, 29–35.

Conti, G., Rostami, A., Scarpini, E., Baron, P., Galimberti, D., Bresolin, N., Contri, M., Palumbo, C., De Pol, A., 2004. Inducible nitric oxide synthase (iNOS) in immune-mediated demyelination and Wallerian degeneration of the rat peripheral nervous system. Exp. Neurol. 187, 350–358.

Gargalovic, P., Dory, L., 2003. Cellular apoptosis is associated with increased caveolin-1 expression in macrophages. J. Lipid Res. 44, 1622–1632.

Ikezu, T., Ueda, H., Trapp, B.D., Nishiyama, K., Sha, J.F., Volonte, D., Galbiati, F., Byrd, A.L., Bassell, G., Serizawa, H., Lane, W.S., Lisanti, M.P., Okamoto, T., 1998. Affinity-purification and characterization of caveolins from the brain: differential expression of caveolin-1, -2, and -3 in brain endothelial and astroglial cell types. Brain Res. 804, 177–192.

Kiss, A.L., Turi, A., Muller, N., Kantor, O., Botos, E., 2002. Caveolae and caveolin isoforms in rat peritoneal macrophages. Review. Micron 33, 75–93.

Lee, Y., Shin, T., 2002. Expression of constitutive endothelial and inducible nitric oxide synthase in the sciatic nerve of Lewis rats with experimental autoimmune neuritis. J. Neuroimmunol. 126, 78–85.

Liu, J., Lee, P., Galbiati, F., Kitsis, R.N., Lisanti, M.P., 2001. Caveolin-1 expression sensitizes fibroblastic and epithelial cells to apoptotic stimulation. Am. J. Physiol.: Cell Physiol. 280, C823–C835.

Mikol, D.D., Scherer, S.S., Duckett, S.J., Hong, H.L., Feldman, E.L., 2002. Schwann cell caveolin-1 expression increases during myelination and decreases after axotomy. Glia 38, 191–199.

Moon, C., Ahn, M., Kim, H., Lee, Y., Koh, C.S., Matsumoto, Y., Shin, T., 2005. Activation of p38 mitogen-activated protein kinase in the early and peak phases of autoimmune neuritis in rat sciatic nerves. Brain Res. 1040, 208–213.

Okamoto, T., Schlegel, A., Scherer, P.E., Lisanti, M.P., 1998. Caveolins, a family of scaffolding proteins for organizing preassembled signaling complexes at the plasma membrane. J. Biol. Chem. 273, 5419–5422.

Shin, T., Lee, Y., Sim, K.B., 2003. Involvement of cyclooxygenase-1 and -2 in the sciatic nerve of rats with experimental autoimmune neuritis. Immunol. Invest. 32, 123–130.

Shin, T., Kim, H., Jin, J.K., Moon, C., Ahn, M., Tanuma, N., Matsumoto, Y., 2005. Expression of caveolin-1, -2, and -3 in the spinal cords of Lewis rats with experimental autoimmune encephalomyelitis. J. Neuroimmunol. 165, 11–20.

Tan, W., Rouen, S., Barkus, K.M., Dremina, Y.S., Hui, D., Christianson, J.A., Wright, D.E., Yoon, S.O., Dobrowsky, R.T., 2003. Nerve growth factor blocks the glucose-induced down-regulation of caveolin-1 expression in Schwann cells via p75 neurotrophin receptor signaling. J. Biol. Chem. 278, 23151–23162.

Williams, T.M., Lisanti, M.P., 2004. The caveolin genes: from cell biology to medicine. Ann. Med. 36, 584–595.

Weishaupt, A., Bruck, W., Hartung, T., Toyka, K.V., Gold, R., 2001. Schwann cell apoptosis in experimental autoimmune neuritis of the Lewis rat and the functional role of tumor necrosis factor-alpha. Neurosci. Lett. 306, 77–80.

Zetti, U.Z., Gold, R., Toyka, K.V., Hartung, H.P., 1996. In situ demonstration of T cell activation and elimination in the peripheral nervous system during experimental autoimmune neuritis in the Lewis rat. Acta Neuropathol. (Berl.) 91, 360–367.

Zhu, W., Mix, E., Nennesmo, I., Adem, A., Zhu, J., 2004. Anti-cytokine autoantibodies in experimental autoimmune neuritis in Lewis rats. Exp. Neurol. 190, 486–494.

Acta Neuropathol (2006) 112: 195–204
DOI 10.1007/s00401-006-0083-7

ORIGINAL PAPER

Naoyuki Tanuma · Hiroshi Sakuma · Atsushi Sasaki
Yoh Matsumoto

Chemokine expression by astrocytes plays a role in microglia/macrophage activation and subsequent neurodegeneration in secondary progressive multiple sclerosis

Received: 29 March 2006 / Revised: 3 May 2006 / Accepted: 4 May 2006 / Published online: 30 May 2006

Abstract The pathological hallmarks of secondary progressive (SP) multiple sclerosis (MS) include slowly expanding demyelination and axonal damage with less inflammation. To elucidate the pathomechanisms of secondary progressive (SP) multiple sclerosis (MS), we have investigated the expression of chemokines, chemokine receptors, matrix metalloproteinase-9 (MMP-9) and immunoglobulins in the demyelinating plaques. Immunohistochemical analysis revealed that numerous hypertrophic astrocytes were observed at the rim, but not in the center, of the chronic active lesions. Microglia/macrophages phagocytosing myelin debris were also found at the lesion border. In contrast, T cell infiltration was minimal in these plaques. Characteristically, at the rim of the lesions, there were abundant immunoreactivities for monocyte chemoattractant protein-1 (MCP-1)/CCL2 and interferon-γ inducible protein-10 (IP-10)/CXCL10 and their receptors, CCR2 and CXCR3, while these immunoreactivities were weak in the center, thus forming a chemokine gradient. Double immunofluorescense staining demonstrated that cellular sources of MCP-1/CCL2 and IP-10/CXCL10 were hypertrophic astrocytes and that both astrocytes and microglia/macrophages expressed CCR2 and CXCR3. MMP-9 was also present at the rim of the lesions. These results suggest that MCP-1/CCL2 and IP-10/CXCL10 produced by astrocytes may activate astrocytes in an autocrine or paracrine manner and direct reactive gliosis followed by migration and activation of microglia/macrophages as effector cells in demyelinating lesions. Targeting chemokines in SPMS may therefore be a powerful therapeutic approach to inhibit lesional expansion.

Keywords Multiple sclerosis · Progression · Immunohistochemistry · Chemokine

N. Tanuma · H. Sakuma · Y. Matsumoto (✉)
Department of Molecular Neuropathology,
Tokyo Metropolitan Institute for Neuroscience,
2-6, Musashidai, Fuchu, Tokyo 183-8526, Japan
E-mail: matyoh@tmin.ac.jp
Tel.: +81-423-253881
Fax: +81-423-218678

A. Sasaki
Department of Human Pathology,
Gunma University Graduate School of Medicine,
3-39-22, Showa-machi, Maebashi, Gunma 371-8511, Japan

Introduction

Multiple sclerosis (MS) is an inflammatory disease of the central nervous system (CNS) that causes demyelinating plaques with glial scar formation. Recent studies have demonstrated that MS is a disease with heterogeneous pathogenetic mechanisms in terms of clinical course, neuropathological and neuroradiological appearance of the lesions and response to therapy [20, 28]. In most patients with MS, the disease begins at about 30 years of age with episodes of acute worsening of neurologic function, followed by a variable degree of recovery between relapses, the relapsing–remitting (RR) phase of the disease. Moreover, in about half of the patients, the clinical course changes from a RR to a secondary progressive (SP) MS after 10 year and almost 90% by 25 years [28]. This shift is a serious problem because once secondary progression begins, patients appear to progress at a uniform rate regardless of how long the disease is present. SPMS responds poorly to medications which are effective in RRMS [7]. Based on pathological examination, it is generally accepted that the pathogenesis of MS consists of inflammatory and neurodegenerative phases [39]. While an inflammatory process plays a central role in reversible demyelination in RRMS, non-remitting clinical disability and disease progression in SPMS is due to degeneration of both the myelin sheath and the axon [4, 5, 40, 46]. The extent of axonal damage correlated with the numbers of macrophages/microglia [17], suggesting that these cells or their toxic products such as tumor necrosis factor-α (TNF-α), nitric oxide (NO) and matrix metalloproteinases (MMPs) are main effectors in this process [3, 9, 16]. Axons can also be damaged by

antibody-mediated destruction via Fc or complement receptors [13, 32, 33]. However, the pathogenesis of neurodegeneration in MS is still a matter of debate.

Chemokines, chemotactic cytokines that selectively recruit specific subsets of leukocytes into tissues, are essential for inflammatory responses [21, 47]. So far, the role of these chemokines in MS has been mainly discussed in terms of inflammatory recruitment of leukocytes into the CNS [15, 37, 41]. For example, interferon-γ inducible protein (IP)-10/CXCL10 is produced by astrocytes and their receptor CXCR3-positive leukocytes migrate into the lesion of MS [2, 36, 38]. Monocyte chemoattractant protein (MCP)-1/CCL2 is also expressed by astrocytes and plays a role in the recruitment and activation of myelin degrading macrophages [26, 35, 42]. However, the effects of these chemokines in the neurodegenerative phase on brain parenchymal cells, in particular astrocytes and microglia, remains to be elucidated.

The purpose of the present study was to analyze in more detail the immunopathological features of SPMS in order to identify factors that are involved in neurodegeneration because the results obtained provide useful information to develop specific immunotherapy against this form of MS. Here, we have investigated the expression of chemokines, MCP-1/CCL2 and IP-10/CXCL10, and their receptor, CCR2 and CXCR3, in the brain from patients with SPMS. Consequently, we found at the rim of the plaques with ongoing demyelination that MCP-1/CCL2 and IP-10/CXCL10 produced by astrocytes and that CCR2 and CXCR3 were abundantly expressed by astrocytes and microglia/macrophages. In contrast, there were weak immunoreactivities for these chemokines and their receptors in the center of the lesions. Thus, along this chemokine gradient, microglia/macrophages expressing CCR2 and CXCR3 were activated. In addition, MMP-9 that is reported to be involved in the lesion formation in MS [6, 8] was predominantly expressed at the rim of the plaque. These findings suggest that chemokine expression by astrocytes plays an important role in activation of microglia/macrophages and expansion of demyelinating lesions in SPMS.

Materials and methods

Patients and tissue samples

The present study was approved by Ethics Committee of Tokyo Metropolitan Institute for Neuroscience and performed on postmortem brain tissues from the UK Multiple Sclerosis Tissue Bank and Department of Human Pathology, Gunma University Graduate School of Medicine. Clinical details of each patient are given in Table 1. Twenty-six tissue blocks from MS patients were studied. Control sections came from two blocks of normal appearing white matter (NAWM) of MS patients (MS58 and MS63 in Table 1) and two biopsied brain tissues, which showed no pathological findings.

Histopathology and classification of multiple sclerosis lesions

Frozen sections, 10 μm thick, were stained with hematoxylin and eosin (HE) and with Luxol Fast Blue (LFB) (Kluever–Barrera's method) for determination of the cell morphology and myelin distribution, respectively. We also used Oil Red O staining for neutral lipid to identify myelin breakdown products. The multiple sclerosis lesions were divided into three categories on the base of the staging system described by De Groot et al. [10] with a few modifications [19]. The detailed classification of

Table 1 Summary of cases utilized for immunohistochemistry and histopathological findings of brain samples

Patients	Diagnosis	Age (years)/sex	Disease duration (years)	Postmortem interval (h)	Number of blocks examined	Number of MS lesions	Lesional activity[a]		
							Active	Chronic active	Chronic inactive
MS38	SPMS	42/F	18	21	6	6	1	2	3
MS53	SPMS	66/M	34	26	1	3			3
MS58	SPMS	51/F	21	15	3	4			4
MS60	SPMS	55/M	43	16	3	3		1	2
MS63	SPMS	66/F	30	13	3	2			2
MS74	SPMS	64/F	36	7	2	3		2	1
MS79	SPMS	49/F	21	7	2	3	1	2	
MS80	SPMS	71/F	34	24	1	1		1	
MS88	SPMS	54/F	20	22	3	4			4
MS114	SPMS	52/F	15	12	1	1			1
MS122	SPMS	44/M	12	16	1	1		1	
05-02	Normal[b]	28/F	NA	Biopsy	1	NA	NA	NA	NA
05-30	Normal[b]	61/M	NA	Biopsy	1	NA	NA	NA	NA
Total					28	31	2	9	20

F female; *M* male; *SPMS* secondary progressive multiple sclerosis; *NA* not applicable

[a] Lesional activity was determined by histological examination and divided into three categories (active, chronic active and chronic inactive) as described in the Materials and methods

[b] Although this specimen was biopsied on suspicion of brain tumor, the result was negative

lesions was as follows: (1) *active*, demyelinating lesion with abundant phagocytic macrophages containing myelin components or neutral lipids; perivascular lymphocytes are present; hypertrophic astrocytes are distributed throughout the demyelinated regions; (2) *chronic active*, hypocellular center contains a few macrophages with some residual lipids; lymphocytes are present in the perivascular cuffs; hypercellular rim contains perivascular and parenchymal (foamy) macrophages and hypertrophic astrocytes; (3) *chronic inactive*, hypocellular lesion, usually containing isomorphic gliosis filling up the demyelinated region with widened extracellular spaces; perivascular and parenchymal phagocytic macrophages are not detectable.

Immunohistochemistry

A single immunoperoxidase staining was performed as previously described [23, 30]. In brief, frozen sections were mounted on slides, air dried, and fixed in ether for 10 min at room temperature. After washing with 0.01 mol/l phosphate-buffered saline (PBS, pH7.4), all slides were incubated overnight with primary antibody (Ab) at 4°C and incubated with horseradish peroxidase (HRP)-labeled secondary Ab (horse anti-goat IgG, Vector, Burlingame, CA) at room temperature for 45 min. The following primary antibodies were used: goat anti-MCP-1/CCL2, goat anti-IP-10/CXCL10, goat anti-CCR2, goat anti-CXCR3, goat anti-MMP-9 (Santa Cruz Biotechnology, Inc., Santa Cruz, CA), rabbit anti-glial fibrillary acidic protein (GFAP), mouse anti-human HLA-DP, DQ, DR (CR3/43, DAKO Japan, Kyoto), mouse anti-CD3 (OKT3, purified from the hybridoma supernatant) Abs. After washing with PBS, sections were incubated with biotinyl tyramide (1:1,000) [1] for 10 min to amplify the immunoreactivity for chemokines (MCP-1/CCL2 and IP-10/CXCL10) or their receptors (CCR2 and CXCR3). We used biotinylated anti-human IgG for detection of IgG deposition on the brain tissue. For other immunostainings, sections were incubated with biotinylated anti-mouse or anti-rabbit IgG (Vector, Burlingame, CA) as secondary Ab. Then, slides were incubated with HRP-labeled avidin–biotin complex (ABC), using VECTSTAIN Elite ABC Kit (Vector). HRP binding sites were detected in 0.005% 3,3-diaminobenzidine and 0.01% hydrogen peroxide. To confirm the specificity of the staining, the primary antibodies were omitted or replaced with normal goat serum or normal mouse IgG. In addition, antibodies against these chemokines/chemokine receptors were absorbed with blocking peptides (Santa Cruz Biotechnology, Inc.,). These controls did not show any specific staining.

Confocal microscopy

To identify the types of cells expressing MCP-1/CCL2, IP-10/CXCL10, CCR2 and CXCR3, double-label immunohistochemistry with GFAP or major histocompatibility complex (MHC) class II molecules was performed. Briefly, frozen sections were air dried and fixed as described above. After washing, sections were incubated overnight at 4°C with the first primary antibody (MCP-1/CCL2, IP-10/CXCL10, CCR2 or CXCR3) and incubated with HRP-labeled horse anti-goat IgG, (Vector) at room temperature for 45 min. After a 10-min application of biotinyl tyramide, the HRP signal was visualized with Alexa Fluor® 488-conjugated streptoavidin (Molecular Probes, Eugene, OR). After washing with PBS, slides were incubated with the second primary antibody (anti-GFAP or anti-HLA DP, DQ, DR) overnight at 4°C and the signal was detected by a 1-h incubation with rhodamine-conjugated anti-rabbit IgG or Cy3-conjugated anti-mouse IgG (Amersham Life Science, Tokyo, Japan). The observation was made using a confocal microscope TCS-SP (Leica, Heidelberg, Germany).

Quantitative analysis of chemokine- and chemokine receptor-positive cells in MS lesions

Quantitative analysis of chemokine- and chemokine receptor-positive cells in MS lesions was performed by two independent observers (N. Tanuma and H. Sakuma). Appropriate areas of the sections were selected according to the demyelinating activity within the lesions. The number of MCP-1/CCL2-, IP-10/CXCL10-, CCR2- and CXCR3-positive cells was determined at least in three standardized microscopic fields of 62,500 μm^2 (defined by a morphometric grid) from each of the distinct lesional areas. In the text and figures, the mean number of cells per mm^2 is given.

Statistics

Data were analyzed with the Student's *t*-test or the nonparametric Mann–Whitney *U* test for two-group comparisons. Reported *P* values were two-tailed and considered significant at *P* value less than 0.05.

Results

We examined 28 brain tissue blocks from 11 MS patients and 2 normal controls (Table 1). Two (MS58 and MS63) of these blocks from MS patients had the NAWM defined as an area, far away from the lesion, which showed no signs of demyelination by histology and the others contained at least one demyelinating lesion. Among 31 lesions of MS, two lesions were classified as active with abundant perivascular lymphocytes, phagocytic macrophages and hypertrophic astrocytes throughout the lesions. Nine lesions were identified as chronic active with hypercellular rims and hypocellular central lesions. The other 20 lesions were classified as chronic inactive, as they were hypocellular without perivascular and parenchymal phagocytic macrophages.

Astrocytes and microglia are activated at the rim of the plaque in chronic active MS

We first characterized the nature of the chronic active lesions in their center, rim and periplaque white matter in patients with SPMS. Representative results are shown in Fig. 1. Consistent with HE and LFB staining, lipid droplets were few in number in the center (Fig. 1a). In sharp contrast, there were numerous lipid-laden foamy macrophages at the rim of the lesions (Fig. 1b), suggesting that active demyelination takes place at this site. In the periplaque area, virtually no lipid deposition was observed (Fig. 1c). In GFAP staining, numerous hypertrophic astrocytes were detected at the rim of the chronic active lesion (Fig. 1e). These astrocytes were also observed both in the center of the lesion and in the periplaque white matter, but were smaller in number and size (Fig. 1d, f). At the rim of the plaque, lipid-laden foamy macrophages were positive for MHC class II antigens (Fig. 1h). MHC class II-positive microgila/macrophages were also detected in the center of the plaque although their shapes were not foamy but more concentrated (Fig. 1g). MHC class II-positive "ramified" microglia were observed in the periplaque white matter outside the plaque (Fig. 1i). Thus, MHC class II-positive microglia/macrophages closer to the lesion site were rounder and larger. These results clearly showed that microglial activation was observed mainly at the lesion border. In these plaques, T cell infiltration was minimal and restricted to the perivascular space of a few blood vessels (Fig. 1j–l). Normal control brains and NAWM of SPMS contained no activated microglia, hypertrophic astrocytes and T cell infiltration (data not shown).

The expression of chemokines and their receptors in different areas of MS lesions

We next analyzed the distribution of MCP-1/CCL2-, IP-10/CXCL10-, CCR2- and CXCR3-immunoreactive cells in the center and rim of the lesions, periplaque white matter and NAWM. The results from chronic active lesions are shown in Fig. 2. MCP-1/CCL2- and IP-10/CXCL10-positive cells were predominantly observed at the rim of the plaques in chronic active lesions rather than in the center (Fig. 2a, c). These immunoreactive cells possessed morphological features of hypertrophic astro-

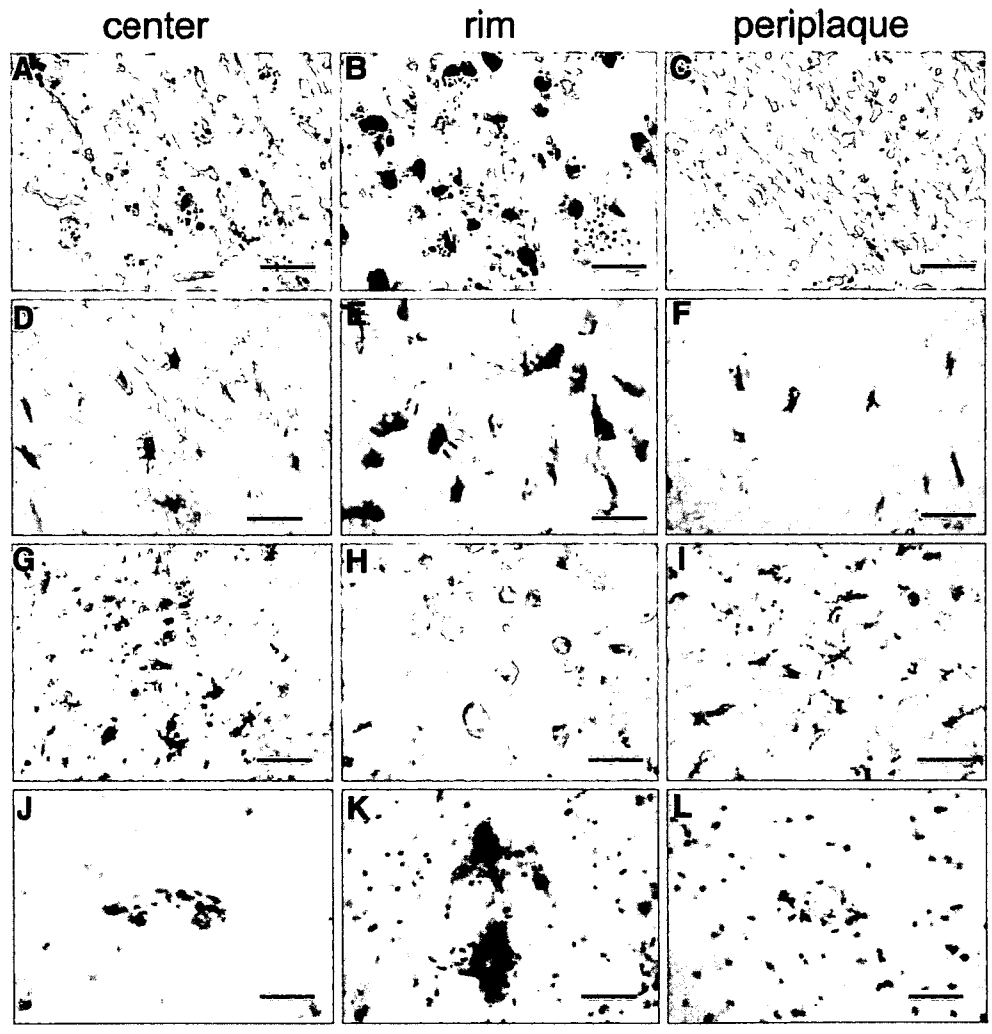

Fig. 1 Astrocytes and microglia are activated at the rim of the plaque in chronic active MS. Lipid-laden macrophages were abundantly observed at the rim of the lesion **b**, but occasionally at the center **a**. No lipid-containing macrophages were detected in periplaque white matters around the lesion **c**. Numerous GFAP-positive hypertrophic astrocytes were detected at the rim of the lesions **e**, while immunoreactivity for GFAP was relatively weak at the center of the lesion **d** and periplaque white matter **f**. In accordance with reactive astrocytes, MHC class II-positive "foamy" microglia/macrophages were observed at the edge of the chronic active lesion **h**, whereas its shape was more concentrated at the center of the plaque **g**. In the periplaque white matter, only MHC class II-positive-"ramified" microglia were observed **i**. T cell infiltration was minimal and restricted to the perivascular space of a few blood vessels **j–l**. **a–c** Oil Red O staining, **d–f** GFAP staining, **g–i** CR3/43 staining, **j–l** OKT3 staining. Scale bar = 50 μm

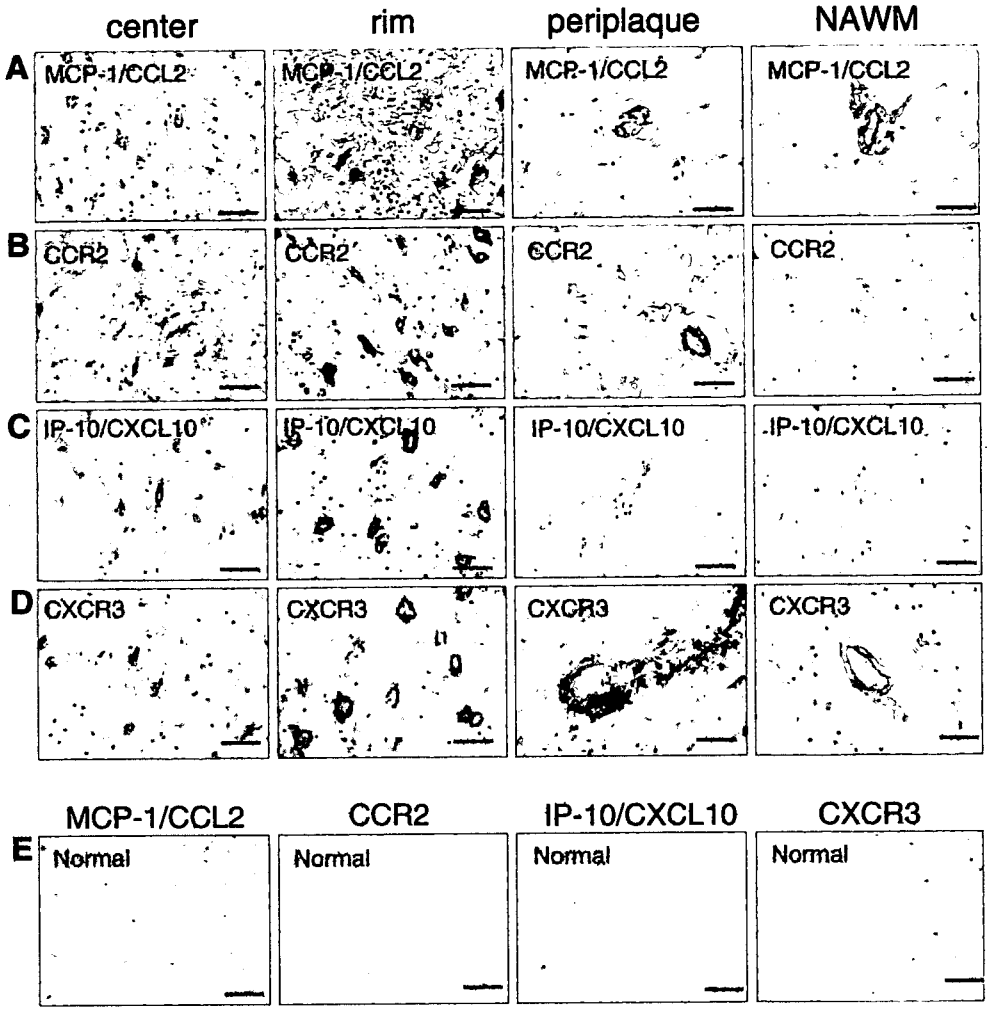

Fig. 2 Immunohistochemistry for MCP-1/CCL2 **a**, CCR2 **b**, IP-10/CXCL10 **c** and CXCR3 **d** in the center, rim, periplaque of chronic active MS lesion, normal appearing white matter (NAWM) and normal control brain **e**. There were abundant immunoreactivities for these chemokines and their receptors at the rim of the lesions with ongoing demyelination, while immunoreactivities for all chemokines and their receptors examined were relatively low at the center of the lesions. In periplaque white matter around the lesion, immunoreactivity for CCR2 **b** was still upregulated. These immunoreactive cells possessed morphological features of astrocytes. In addition, immunohistochemistry for MCP-1/CCL2 **a**, CCR2 **b** and CXCR3 **d** showed staining of the blood vessel endothelium. MCP-1/CCL2 and CXCR3 were constitutively expressed on the blood vessel endothelium in NAWM. Normal control brain showed no expression of MCP-1/CCL2, IP-10/CXCL10, CCR2 and CXCR3 **e**. Scale bar = 50 μm

cytes. Similarly, the corresponding chemokine receptors, CCR2- and CXCR3-positive cells were seen mainly at the rim of the plaques (Fig. 2b, d). Although these plaques contained some perivascular cuffs, all these lymphocytes were negative for CXCR3 (data not shown). In the periplaque white matter outside of the plaques, immunoreactivity for CCR2 (Fig. 2b) was still upregulated whereas there were no immunoreactivities except for MCP-1-positive (Fig. 2a) and CXCR3-positive (Fig. 2d) endothelial cells in these lesions. In NAWM, immunoreactivities for MCP-1/CCL2 and CXCR3 were positive in endothelial cells (Fig. 2a,d). We also examined the expression of chemokines and their receptors in normal brains. Normal brains did not express MCP-1/CCL2, IP-10/CXCL10, CCR2 and CXCR3 (Fig. 2e), while immunoreactivities for MCP-1/CCL2 and CXCR3 were positive in endothelial cells in NAWM (Fig. 2a, d). Quantitative analysis of chemokine- and chemokine receptor-positive cells clearly demonstrated that the numbers of all the positive cells at the rim were greater than that in the center of chronic active lesions (Fig. 3). The number of MCP-1/CCL2- (Fig. 3a), CCR2- (Fig. 3b), IP-10/CXCL10- (Fig. 3c) and CXCR3- (Fig. 3d) positive cells at the rim of the lesions were significantly larger than that in the center of the lesions. These findings strongly suggest that astrocytes produce MCP-1/CCL2 and IP-10/CXCL10 mainly at the lesion borders, forming a "chemokine gradient" from the center to rim within the plaque in SPMS.

Table 2 summarizes the results of chemokine and chemokine receptor staining of the active, chronic active and chronic inactive lesions. In the chronic inactive lesion, there was a hypocellular center where none of cells expressed MCP-1/CCL2, CCR2, IP-10/CXCL10 and CXCR3. At the rim of these lesions, there were a few MCP-1/CCL2- and CXCR3-positive cells. In contrast to chronic active lesions, there were no IP-10/CXCL10- and CCR2-positive cells in chronic inactive lesions (Table 2).

Astrocytes express both chemokines and chemokine receptors but microglia express only chemokine receptors in the chronic active MS lesions

To determine the type of cells that produce MCP-1/CCL2 and IP-10/CXCL10 and cells expressing their receptor, CCR2 and CXCR3, we performed double immunofluorescense staining with astrocyte and microglia/macrophage markers. The results are shown in Fig. 4.

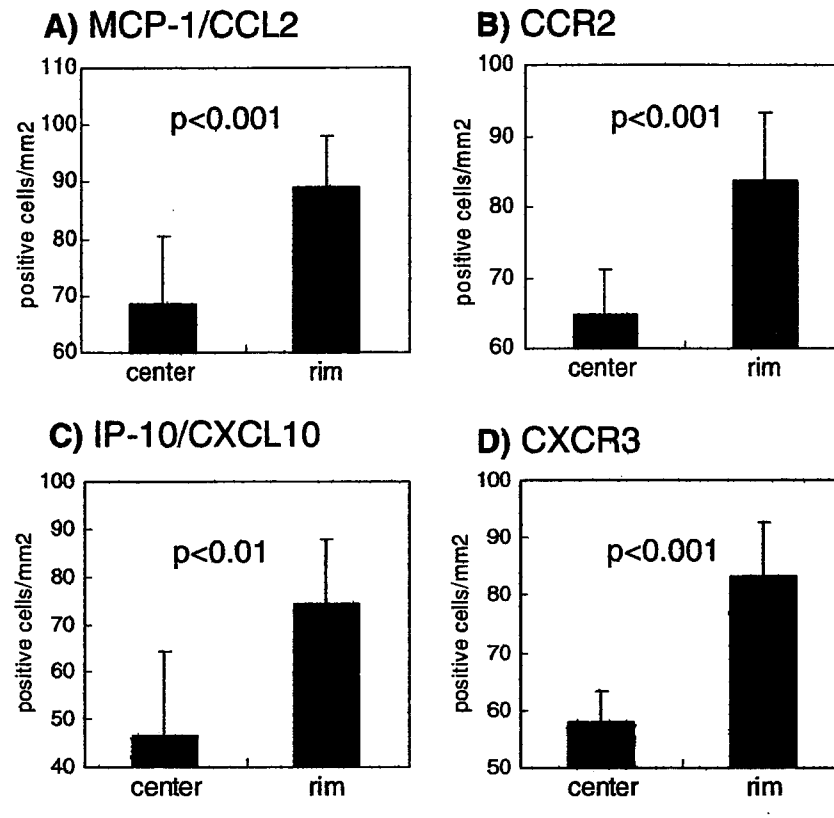

Fig. 3 Quantification of MCP-1/CCL2- **a**, CCR2- **b**, IP-10/CXCL10- **c** and CXCR3- **d** positive cells in chronic active MS lesion. The number of positive cells was determined in at least three standardized fields of 62,500 μm^2 (defined by a morphometric grid) from each of the distinct lesional areas. Data are expressed as mean ± SD (cells/mm^2). The number of all chemokine- and chemokine receptor-positive cells at the rim of the lesion was significantly higher than that at the center of the lesion

Table 2 Expression of chemokines and chemokine receptors in MS lesions

Chemokines and chemokine receptors	Active[a]–chronic active[b]			Chronic inactive[c]		
	Center	Rim	Periplaque	Center	Rim	Periplaque
MCP-1	++	+++	+	–	+	+
IP-10	++	+++	–	–	–	–
CCR2	++	+++	+	–	–	–
CXCR3	++	+++	+	–	+	+

– = no immunoreactive cells, + = sporadic or a few positive cells, ++ = moderate positive cells in the same area, +++ = abundant immunoreactivity

[a] Active is defined as the demyelinating lesion with abundant phagocytic macrophages containing myelin components or neutral lipids; perivascular lymphocytes are present; hypertrophic astrocytes are distributed throughout the demyelinated regions

[b] Chronic active is defined as the lesion with hypocellular center containing a few macrophages with some residual lipids; lymphocytes are present in the perivascular cuffs; hypercellular rim contains perivascular and parenchymal (foamy) macrophages and hypertrophic astrocytes

[c] Chronic inactive is defined as the hypocellular lesion, usually containing isomorphic gliosis filling up the demyelinated region with widened extracellular spaces; perivascular and parenchymal phagocytic macrophages are not detectable

As clearly demonstrated in Fig. 4a–l, GFAP-positive astrocytes expressed both MCP-1/CCL2 (Fig. 4c, arrows) and IP-10/CXCL10 (Fig. 4i, arrow heads), whereas CR3/43-positive microglia/macrophages were completely negative for these chemokines (Fig. 4f, l). With regard to chemokine receptors (Fig. 4m–x), both CCR2 and CXCR3 were expressed on astrocytes (Fig. 4o, u) and microglia/macrophages (Fig. 4r, x). These findings strongly suggest that hypertrophic astrocytes produce MCP-1/CCL2 and IP-10/CXCL10 and also express their receptors, while microglia/macrophages do not produce these chemokines and only express the receptors.

MMP-9 are predominantly expressed at the rim of the lesion

MMPs are considered to be one of the toxic substances for demyelination and axonal injury [8, 9, 12, 22, 43]. To determine the involvement of MMPs in microglia/macrophages-mediated demyelination and axonal damage, we examined the localization of MMP-9 in the MS lesion, because MMP-9 plays a role in blood–brain barrier (BBB) breakdown, myelin degradation and axonal damage [6, 27, 34]. We found that MMP-9 was predominantly expressed at the rim of the plaques in chronic active lesions (Fig. 5b) rather than in the center (Fig. 5a).

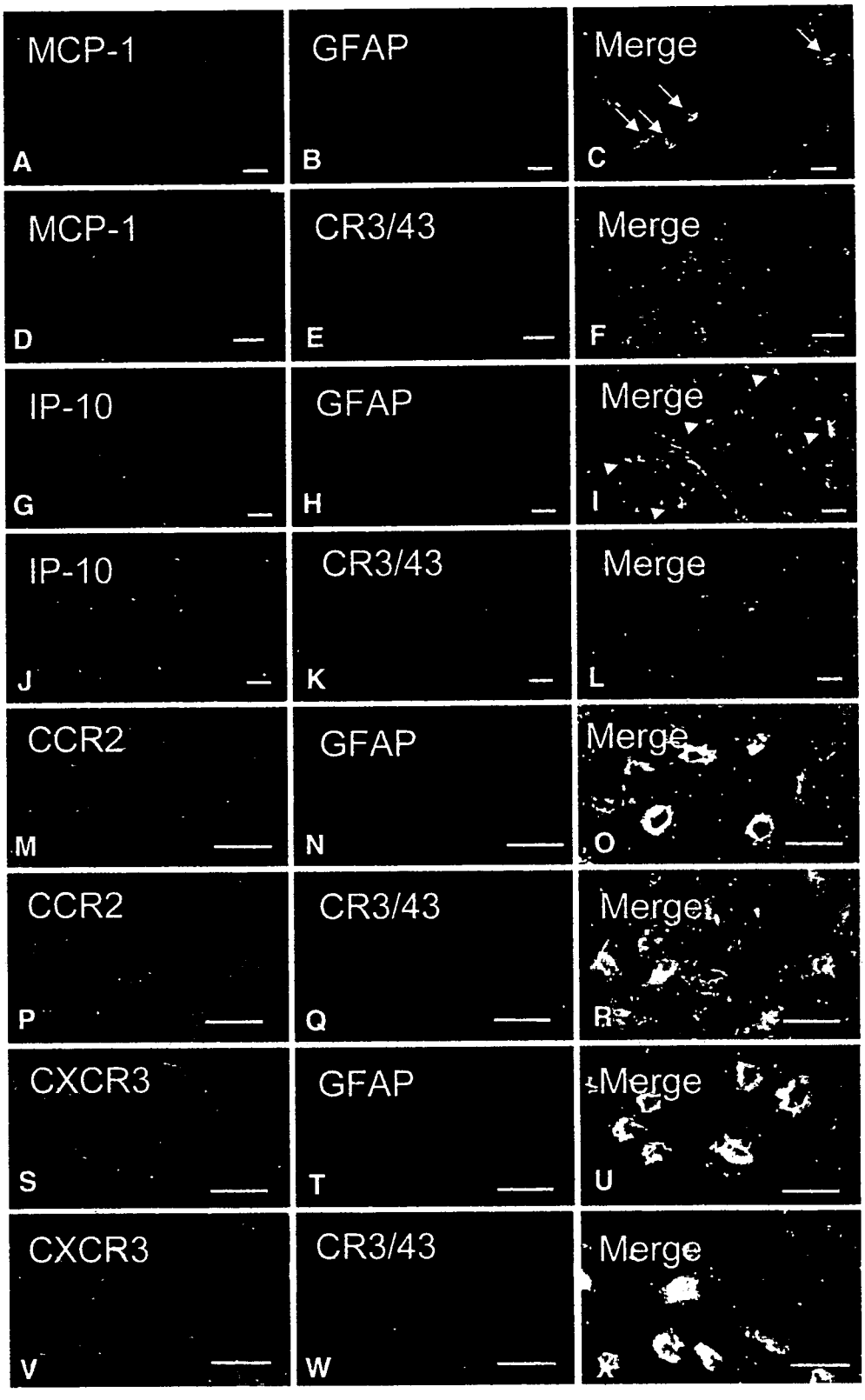

Fig. 4 Identification of the type of cells expressing chemokines (**a–l**) and chemokine receptors (**m–x**). Double immunofluorescense staining for MCP-1/CCL2 (*green*) (**a, d**), IP-10/CXCL10 (*green*) (**g, j**), CCR2 (M, P) and CXCR3 (*green*) (**s, v**) with GFAP (*red*) (**b, h, n** and **t**) and MHC class II, CR3/43 (*red*) (**e, k, q** and **w**) in lesions from patients with SPMS. **c, f, i** and **l** are merged images of **a, b; d, e; g, h** and **j, k**, respectively. Both MCP-1/CCL2 and IP-10/CXCL10 were expressed by astrocytes (**c** *arrows* and **i** *arrow heads*), but was not expressed by microglia (**f** and **l**). **o, r, u** and **x** are merged images of **m, n; p, q; s, t,** and **v, w**, respectively. CCR2 and CXCR3 were expressed by both astrocytes (**o, u**) and microglia (**r, x**). Scale bar = 50 μm

In the periplaque white matter outside of the plaques, immunoreactivity for MMP-9 was weakly detected (Fig. 5c). We also determined the IgG deposition in the lesion. Unlike MMP-9, IgG immunoreactivities were present in both the center and the rim of the plaque (Fig. 5d, e). In the periplaque white matter, faint to moderate staining was observed around blood vessels (Fig. 5f). Absorption of anti-MMP-9 and anti-human IgG with MMP-9 peptide and human sera, respectively, resulted in negative staining, indicating that these immu-

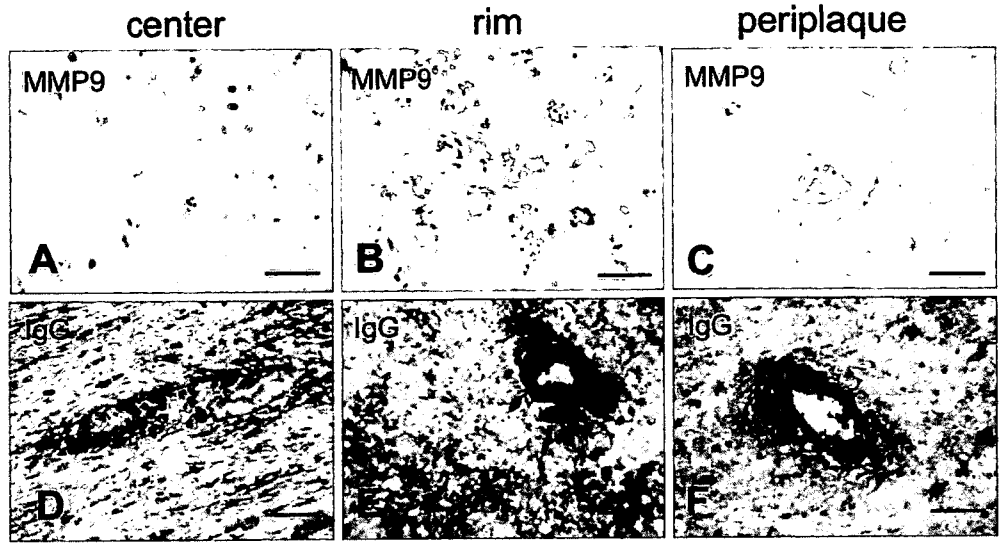

Fig. 5 Immunohistochemistry for MMP-9 (**a–c**) and IgG (**d–f**) in the center (**a, d**), rim (**b, e**) and periplaque (**c, f**) of chronic active MS lesion. The expression of MMP-9 was predominantly observed at the rim **b** rather than in the center **a**. In the periplaque white matter outside of the plaques, immunoreactivity for MMP-9 was weakly detected **c**. In contrast, both the center and the rim of the plaque showed moderately intense immunoreactivity for IgG (**d, e**). In periplaque white matter, faint to moderately intense staining was observed around blood vessels **f**. Scale bar = 50 μm

noreactivities were specific (data not shown). These results suggest that activated microglia might produce MMP-9 at the rim of the plaque and contribute to slowly progressive expanding lesions.

Discussion

SPMS is characterized by irreversible neurological impairment without remission. Pathologically, SPMS has a slowly expanding demyelinating lesion with only modest inflammatory cell cuffing. This ongoing demyelinating lesion, namely, "progressive plaque" includes linear group of microglia engaging short segments of disrupted myelin that are associated with deposits of C3d [32]. Axonal damage is also considered to be a major cause of secondary progression with irreversible neurological impairment [4, 11, 40]. Previous studies suggested that not only T cells [17] but also microglia/macrophages and their toxic products such as tumor necrosis factor-α (TNF-α), nitric oxide (NO) and MMPs are main effectors in this process [3, 8, 16]. However, the mechanisms of microglia/macrophage activation and subsequent toxic substance production in "progressive" or chronic active plaques remain unknown.

In the present study, we have investigated the expression of chemokines, MCP-1/CCL2 and IP-10/CXCL10, and their receptor, CCR2 and CXCR3, in the brain of patients with SPMS to elucidate the pathomechanisms of secondary progression of the MS lesion where lymphocyte infiltration is minimal or absent. As clearly shown here, there were abundant immunoreactivities for MCP-1/CCL2, IP-10/CXCL10, CCR2 and CXCR3 at the rim of the lesions with ongoing demyelination, whereas these immunoreactivities were relatively weak in the center of the lesions, forming a chemokine gradient. Double immunofluorescense staining revealed that both chemokines and their receptors were expressed by hypertrophic astrocytes, while only chemokine receptors were expressed by MHC class II-positive microglia/macrophages. It should be emphasized that there was no evidence of chemokine production by microglia/macrophages. Although it was stated in a previous report [35] that MCP-1/CCL2 was expressed by astrocytes and macrophages within acute MS lesions, we demonstrated using double immunofluorescense staining that microglia/macrophages were always negative in both active and chronic active lesions. In addition, the previous studies demonstrated that CXCR3 is expressed by perivascular lymphocytes mainly in acute MS and/or relapsing–remitting MS [36, 37]. However, our study revealed that CXCR3 was not expressed by perivascular lymphocytes in chronic MS lesions, especially with minimal lymphocyte infiltration. Our result suggests that T lymphocytes are not crucial any longer in this chronic stage. The results obtained in the present study also suggest that chemokines produced by astrocytes play a role in astrocytic migration and proliferation in an autocrine or paracrine manner, resulting in reactive astrogliosis observed at the rim of the plaque in SPMS. It is likely that CCR2- or CXCR3-positeve microglia can also migrate into the rim in response to MCP-1/CCL2 and IP-10/CXCL10 produced by astrocytes. Finally, as shown here, activated microglia may secrete toxic substances such as MMP-9, one of final effectors for demyelination [8] and axonal injury [12, 27]. Recently, Omari et al. [31] reported that chemokines produced by astrocytes induces the recruitment of oligodendrocytes which expressed different CXC chemokine receptors and subsequent remyelination in MS. Thus, chemokines play an important role, not only in the leukocytes recruitment into the inflammatory site, but also in the recruitment of brain parenchymal cells, in particular astrocytes, microglia and oligodendrocytes.

We were also interested in the distribution of IgG in and around the plaque because IgGs, especially autoantibodies to myelin oligodendrocyte glycoprotein (MOG), play an important role in demyelination under a certain circumstance [13, 20, 33]. However, the recent study by

Lalive et al. [18] demonstrated that native MOG-specific IgGs, which induce demyelination were most frequently found in serum of clinically isolated syndromes and RRMS, while only marginally in SPMS, suggesting that native MOG-specific IgGs may be implicated in the early pathogenesis of MS. In this study, we found that moderately intense immunoreactivities for IgG were evenly distributed both in the center and at the rim of the plaque. O'Connor et al. [29] demonstrated that the majority of CNS samples from patients with MS yielded substantially greater quantities of IgG than those from control cases by eluting IgG from plaque tissue. In addition, they also demonstrated that IgG derived from MS plaque tissue contains autoantibodies that recognize the folded (native) human MOG proteins. Thus, antibodies from inflamed CNS tissue recognize MOG. Although we did not examine the distribution of MOG-specific IgG and further investigation will be required, our results suggest that anti-myelin antibodies may not be involved in microglial activation and MMP-9 secretion at the rim of the plaque at the later disease stage. Prineas et al. [32] showed that the ongoing demyelinating lesions in SPMS include C3d deposition but this is an antibody-independent process. Taken together, it is likely that Ab-mediated activation of microglia may be less implicated in the mechanisms for lesion expansion in SPMS.

Recently, evidence is accumulating that chemokines also play an important role, not only in autoimmune diseases, but also in neurodegenerative disorders. In amyotrophic lateral sclerosis (ALS), the MCP-1/CCL2 level in cerebrospinal fluid was significantly increased compared to the control subjects [14, 44]. In ALS spinal cord tissue, MCP-1/CCL2 protein was expressed in glia, probably astrocytes [14]. Thus, MCP-1/CCL2 may recruit both astrocytes and microglia into the lesion site and promote neurodegeneration. These results together with our findings suggest that the neurodegenerative phase of MS and of neurodegenerative disorders such as ALS have common disease processes in the lesion formation. These findings also suggest that chemokines and chemokine receptors could be targets of therapies. We recently demonstrated that gene therapy with decoy chemokine receptor DNAs encoding the binding sites of the CCR2 and CXCR3 molecules prevent the disease progression of experimental autoimmune myocarditis and subsequent dilated cardiomyopathy [25]. In addition, chronic relapsing experimental autoimmune encephalomyelitis (EAE), which was recently produced by us, was effectively inhibited by anti-macrophage migration therapy using decoy chemokine and chemokine receptor DNA therapy [24]. It is also shown that deletion of macrophage-inflammatory protein (MIP)-1α/CCL3 retards neurodegeneration in mice with Sandhoff disease, a lysosomal storage disorder caused by a deficiency of β-hexosaminidases A and B [45]. The result indicates that the pathogenesis of Sandhoff disease involves an increase in MIP-1α/CCL3 that induces monocytes to infiltrate the CNS, expand the activated microglia/macrophages, and trigger apoptosis of neurons. Together, chemokines could be possible targets for therapies to slow the neurodegenerative phase in autoimmune and degenerative disorders.

In summary, we have investigated the expression of chemokines and chemokine receptors in the brain from patients with SPMS and found that MCP-1/CCL2, IP-10/CXCL10 produced by astrocytes and their receptors, CCR2, CXCR3, were abundantly expressed by astrocytes and microglia/macrophages at the rim of the lesions with ongoing demyelination. Our findings suggest that these chemokine–chemokine receptor pairs may contribute to a neurodegenerative phase of MS through recruitment of astrocytes and microglia into the site of expanding lesions. Targeting chemokines in a neurodegenerative phase of MS may therefore be a possible therapeutic approach to inhibit lesional expansion.

Acknowledgments The authors thank Yoko Kawazoe for technical assistance. MS brain tissue samples were supplied by the UK Multiple Sclerosis Tissue Bank. This work was supported in part by grants from the Ministry of Education, Culture, Sports, Science and Technology, Japan.

References

1. Adams JC (1992) Biotin amplification of biotin and horseradish peroxidase signals in histochemical stains. J Histochem Cytochem 40:1457–1463
2. Balashov KE, Rottman JB, Weiner HL, Hancock WW (1999) CCR5(+) and CXCR3(+) T cells are increased in multiple sclerosis and their ligands MIP-1alpha and IP-10 are expressed in demyelinating brain lesions. Proc Natl Acad Sci USA 96:6873–6878
3. Bitsch A, da Costa C, Bunkowski S, Weber F, Rieckmann P, Bruck W (1998) Identification of macrophage populations expressing tumor necrosis factor-alpha mRNA in acute multiple sclerosis. Acta Neuropathol (Berl) 95:373–377
4. Bitsch A, Schuchardt J, Bunkowski S, Kuhlmann T, Bruck W (2000) Acute axonal injury in multiple sclerosis. Correlation with demyelination and inflammation. Brain 123:1174–1183
5. Bjartmar C, Kinkel RP, Kidd G, Rudick RA, Trapp BD (2001) Axonal loss in normal-appearing white matter in a patient with acute MS. Neurology 57:1248–1252
6. Chandler S, Coates R, Gearing A, Lury J, Wells G, Bone E (1995) Matrix metalloproteinases degrade myelin basic protein. Neurosci Lett 201:223–226
7. Confavreux C, Vukusic S, Moreau T, Adeleine P (2000) Relapses and progression of disability in multiple sclerosis. N Engl J Med 343:1430–1438
8. Cossins JA, Clements JM, Ford J, Miller KM, Pigott R, Vos W, Van der Valk P, De Groot CJ (1997) Enhanced expression of MMP-7 and MMP-9 in demyelinating multiple sclerosis lesions. Acta Neuropathol (Berl) 94:590–598
9. Cuzner ML, Gveric D, Strand C, Loughlin AJ, Paemen L, Opdenakker G, Newcombe J (1996) The expression of tissue-type plasminogen activator, matrix metalloproteases and endogenous inhibitors in the central nervous system in multiple sclerosis: comparison of stages in lesion evolution. J Neuropathol Exp Neurol 55:1194–1204
10. De Groot CJ, Bergers E, Kamphorst W, Ravid R, Polman CH, Barkhof F, van der Valk P (2001) Post-mortem MRI-guided sampling of multiple sclerosis brain lesions: increased yield of active demyelinating and (p)reactive lesions. Brain 124:1635–1645
11. DeLuca GC, Ebers GC, Esiri MM (2004) Axonal loss in multiple sclerosis: a pathological survey of the corticospinal and sensory tracts. Brain 127:1009–1018

12. Diaz-Sanchez M, Williams K, Deluca GC, Esiri MM (2006) Protein co-expression with axonal injury in multiple sclerosis plaques. Acta Neuropathol (Berl) 111:289–299
13. Genain CP, Cannella B, Hauser SL, Raine CS (1999) Identification of autoantibodies associated with myelin damage in multiple sclerosis. Nat Med 5:170–175
14. Henkel JS, Engelhardt JI, Siklos L, Simpson EP, Kim SH, Pan T, Goodman JC, Siddique T, Beers DR, Appel SH (2004) Presence of dendritic cells, MCP-1, and activated microglia/macrophages in amyotrophic lateral sclerosis spinal cord tissue. Ann Neurol 55:221–235
15. Kivisakk P, Trebst C, Liu Z, Tucky BH, Sorensen TL, Rudick RA, Mack M, Ransohoff RM (2002) T-cells in the cerebrospinal fluid express a similar repertoire of inflammatory chemokine receptors in the absence or presence of CNS inflammation: implications for CNS trafficking. Clin Exp Immunol 129:510–518
16. Koeberle PD, Ball AK (1999) Nitric oxide synthase inhibition delays axonal degeneration and promotes the survival of axotomized retinal ganglion cells. Exp Neurol 158:366–381
17. Kuhlmann T, Lingfeld G, Bitsch A, Schuchardt J, Bruck W (2002) Acute axonal damage in multiple sclerosis is most extensive in early disease stages and decreases over time. Brain 125:2202–2212
18. Lalive PH, Menge T, Delarasse C, Della Gaspera B, Pham-Dinh D, Villoslada P, von Budingen HC, Genain CP (2006) Antibodies to native myelin oligodendrocyte glycoprotein are serologic markers of early inflammation in multiple sclerosis. Proc Natl Acad Sci USA 103:2280–2285
19. Lassmann H, Raine CS, Antel J, Prineas JW (1998) Immunopathology of multiple sclerosis: report on an international meeting held at the Institute of Neurology of the University of Vienna. J Neuroimmunol 86:213–217
20. Lucchinetti C, Bruck W, Parisi J, Scheithauer B, Rodriguez M, Lassmann H (2000) Heterogeneity of multiple sclerosis lesions: implications for the pathogenesis of demyelination. Ann Neurol 47:707–717
21. Luster AD (1998) Chemokines–chemotactic cytokines that mediate inflammation. N Engl J Med 338:436–445
22. Maeda A, Sobel RA (1996) Matrix metalloproteinases in the normal human central nervous system, microglial nodules, and multiple sclerosis lesions. J Neuropathol Exp Neurol 55:300–309
23. Matsumoto Y, Fujiwara M (1987) The immunopathology of adoptively transferred experimental allergic encephalomyelitis (EAE) in Lewis rats. Part 1. Immunohistochemical examination of developing lesion of EAE. J Neurol Sci 77:35–47
24. Matsumoto Y, Tsukada Y, Miyakoshi A, Sakuma H, Kohyama K (2004) C protein-induced myocarditis and subsequent dilated cardiomyopathy: rescue from death and prevention of dilated cardiomyopathy by chemokine receptor DNA therapy. J Immunol 173:3535–3541
25. Matsumoto Y, Sakuma H, Miyakoshi A, Tsukada Y, Kohyama K, Park IK, Tanuma N (2005) Characterization of relapsing autoimmune encephalomyelitis and its treatment with decoy chemokine receptor genes. J Neuroimmunol 170:49–61
26. McManus CM, Brosnan CF, Berman JW (1998) Cytokine induction of MIP-1 alpha and MIP-1 beta in human fetal microglia. J Immunol 160:1449–1455
27. Newman TA, Woolley ST, Hughes PM, Sibson NR, Anthony DC, Perry VH (2001) T-cell- and macrophage-mediated axon damage in the absence of a CNS-specific immune response: involvement of metalloproteinases. Brain 124:2203–2214
28. Noseworthy JH, Lucchinetti C, Rodriguez M, Weinshenker BG (2000) Multiple sclerosis. N Engl J Med 343:938–952
29. O'Connor KC, Appel H, Bregoli L, Call ME, Catz I, Chan JA, Moore NH, Warren KG, Wong SJ, Hafler DA, Wucherpfennig KW (2005) Antibodies from inflamed central nervous system tissue recognize myelin oligodendrocyte glycoprotein. J Immunol 175:1974–1982
30. Ohmori K, Hong Y, Fujiwara M, Matsumoto Y (1992) In situ demonstration of proliferating cells in the rat central nervous system during experimental autoimmune encephalomyelitis. Evidence suggesting that most infiltrating T cells do not proliferate in the target organ. Lab Invest 66:54–62
31. Omari KM, John GR, Sealfon SC, Raine CS (2005) CXC chemokine receptors on human oligodendrocytes: implications for multiple sclerosis. Brain 128:1003–1015
32. Prineas JW, Kwon EE, Cho ES, Sharer LR, Barnett MH, Oleszak EL, Hoffman B, Morgan BP (2001) Immunopathology of secondary-progressive multiple sclerosis. Ann Neurol 50:646–657
33. Raine CS, Cannella B, Hauser SL, Genain CP (1999) Demyelination in primate autoimmune encephalomyelitis and acute multiple sclerosis lesions: a case for antigen-specific antibody mediation. Ann Neurol 46:144–160
34. Rosenberg GA, Dencoff JE, Correa N, Jr., Reiners M, Ford CC (1996) Effect of steroids on CSF matrix metalloproteinases in multiple sclerosis: relation to blood–brain barrier injury. Neurology 46:1626–1632
35. Simpson JE, Newcombe J, Cuzner ML, Woodroofe MN (1998) Expression of monocyte chemoattractant protein-1 and other beta-chemokines by resident glia and inflammatory cells in multiple sclerosis lesions. J Neuroimmunol 84:238–249
36. Simpson JE, Newcombe J, Cuzner ML, Woodroofe MN (2000) Expression of the interferon-gamma-inducible chemokines IP-10 and Mig and their receptor, CXCR3, in multiple sclerosis lesions. Neuropathol Appl Neurobiol 26:133–142
37. Sorensen TL, Tani M, Jensen J, Pierce V, Lucchinetti C, Folcik VA, Qin S, Rottman J, Sellebjerg F, Strieter RM, Frederiksen JL, Ransohoff RM (1999) Expression of specific chemokines and chemokine receptors in the central nervous system of multiple sclerosis patients. J Clin Invest 103:807–815
38. Sorensen TL, Trebst C, Kivisakk P, Klaege KL, Majmudar A, Ravid R, Lassmann H, Olsen DB, Strieter RM, Ransohoff RM, Sellebjerg F (2002) Multiple sclerosis: a study of CXCL10 and CXCR3 co-localization in the inflamed central nervous system. J Neuroimmunol 127:59–68
39. Steinman L (2001) Multiple sclerosis: a two-stage disease. Nat Immunol 2:762–764
40. Trapp BD, Peterson J, Ransohoff RM, Rudick R, Mork S, Bo L (1998) Axonal transection in the lesions of multiple sclerosis. N Engl J Med 338:278–285
41. Trebst C, Staugaitis SM, Tucky B, Wei T, Suzuki K, Aldape KD, Pardo CA, Troncoso J, Lassmann H, Ransohoff RM (2003) Chemokine receptors on infiltrating leucocytes in inflammatory pathologies of the central nervous system (CNS). Neuropathol Appl Neurobiol 29:584–595
42. Van Der Voorn P, Tekstra J, Beelen RH, Tensen CP, Van Der Valk P, De Groot CJ (1999) Expression of MCP-1 by reactive astrocytes in demyelinating multiple sclerosis lesions. Am J Pathol 154:45–51
43. Vos CM, van Haastert ES, de Groot CJ, van der Valk P, de Vries HE (2003) Matrix metalloproteinase-12 is expressed in phagocytotic macrophages in active multiple sclerosis lesions. J Neuroimmunol 138:106–114
44. Wilms H, Sievers J, Dengler R, Bufler J, Deuschl G, Lucius R (2003) Intrathecal synthesis of monocyte chemoattractant protein-1 (MCP-1) in amyotrophic lateral sclerosis: further evidence for microglial activation in neurodegeneration. J Neuroimmunol 144:139–142
45. Wu YP, Proia RL (2004) Deletion of macrophage-inflammatory protein 1 alpha retards neurodegeneration in Sandhoff disease mice. Proc Natl Acad Sci USA 101:8425–8430
46. Wujek JR, Bjartmar C, Richer E, Ransohoff RM, Yu M, Tuohy VK, Trapp BD (2002) Axon loss in the spinal cord determines permanent neurological disability in an animal model of multiple sclerosis. J Neuropathol Exp Neurol 61:23–32
47. Zlotnik A, Yoshie O (2000) Chemokines: a new classification system and their role in immunity. Immunity 12:121–127

ELSEVIER

Journal of the Neurological Sciences 249 (2006) 145–152

Journal of the Neurological Sciences

www.elsevier.com/locate/jns

Characterization of the T cell receptor repertoire in the Japanese neuromyelitis optica: T cell activity is up-regulated compared to multiple sclerosis

Yoko Warabi [a,b], Kohichi Yagi [a], Hideaki Hayashi [a], Yoh Matsumoto [b,*]

[a] *Department of Neurology, Tokyo Metropolitan Neurological Hospital, Tokyo, Japan*
[b] *Department of Molecular Neuropathology, Tokyo Metropolitan Institute for Neuroscience, 2-6 Musashidai Fuchu, Tokyo 183-8526, Japan*

Received 15 February 2006; accepted 6 June 2006
Available online 24 July 2006

Abstract

To characterize T cell immunity in Japanese neuromyelitis optica (NMO), we examined the T cell receptor (TCR) repertoire in NMO patients with complementarity-determining region 3 (CDR3) spectratyping and compared the results with those from multiple sclerosis (MS) patients and healthy subjects. Both NMO and MS patients had a larger number of clonally expanded Vβ genes than healthy subjects. Moreover, NMO patients had a significantly larger number of expanded Vβs than MS patients. The detailed analysis revealed that Vβ1 and Vβ13 were significantly activated in NMO than MS. These results reflected unique pathophysiology of Japanese NMO, which is distinguishable from that of MS. Furthermore, longitudinal examinations of the TCR repertoire demonstrated that the number of clonally expanded Vβs in NMO correlates with the Kurtzke Expanded disability status scale (EDSS). Although the activation pattern of the TCR repertoire in relapsing-remitting MS (RRMS) was similar to that in NMO, secondary progressive MS (SPMS) patients with longer disease durations and higher EDSS scores consistently had a smaller number of clonally expanded Vβs than RRMS patients. Detailed TCR investigations will provide useful information to evaluate the clinical and immunological status of NMO and MS and to develop effective immunotherapies.

Keywords: Neuromyelitis optica; Multiple sclerosis; T cell receptor; Complementarity-determining region 3; T cell immunity; EDSS

1. Introduction

The clinical features of central nervous demyelinating diseases in Japan are somewhat different from those in western countries. One of the characteristic features is that there are many patients with neuromyelitis optica (NMO), which is also referred to as the optic-spinal form of multiple sclerosis (OS-MS) [1–3]. In a previous report, we demonstrated with complementarity-determining region 3 (CDR3) spectratyping that T cells in the peripheral blood lymphocytes (PBL) and CSF of multiple sclerosis (MS) patients showed frequent expansions of particular Vβs [4]. While this finding suggests that T cells showing clonal expansions are associated with the development of MS, the importance of the T cell immunity in the pathomechanism of NMO remains to be elucidated.

So far, a number of clinical and pathophysiological differences between NMO and MS have been reported. First, lesions in NMO are limited to the optic nerve and spinal cord. The neuropathological features of NMO are characterized by the presence of necrotic lesions in the spinal cord rather than demyelination [5]. Furthermore, NMO are characterized by a female preponderance and an absence of oligoclonal IgG bands [6]. DPB1*0501 is reported to be associated with OS-MS/NMO in Japan [7]. Finally, the levels of chemokines in the sera and cerebrospinal fluid (CSF) are different between NMO and MS. CCL2/MCP-1 in

* Corresponding author. Tel.: +81 42 325 3881x4719; fax: +81 42 321 8678.
E-mail address: matyoh@tmin.ac.jp (Y. Matsumoto).

0022-510X/$ - see front matter © 2006 Elsevier B.V. All rights reserved.
doi:10.1016/j.jns.2006.06.011